Front. Mech. Eng. 2025, 20(1): 1
https://doi.org/10.1007/s11465-024-0817-z

RESEARCH ARTICLE

Tribological evaluation of Al_2O_3/GO/ZnO tripartite hybrid based nanofluid for grinding Ti-6Al-4V alloy with minimum quantity lubrication

Yusuf Suleiman DAMBATTA[a,b,f], Benkai LI[a], Yanbin ZHANG[a], Min YANG[a], Peiming XU[c], Wei WANG[c], Zongming ZHOU[d], Yuying YANG[e], Lan DONG[f], Changhe LI (✉)[a]

[a] *School of Mechanical and Automotive Engineering, Qingdao University of Technology, Qingdao 266520, China*
[b] *Mechanical Engineering Department, Ahmadu Bello University, Zaria 810106, Nigeria*
[c] *Taishan Sports Industry Group Co., Ltd., Dezhou 253600, China*
[d] *Qingdao Hanergy Lubrication Technology Co., Ltd., Qingdao 266000, China*
[e] *Qilu University of Technology, Jinan 250316, China*
[f] *Qingdao Binhai University, Qingdao 266540, China*

✉ *Corresponding author. Email: sy_lichanghe@163.com (Changhe LI)*

ABSTRACT Machining-induced damages encountered during the grinding of titanium alloys are a major setback for processing different components from these materials. Recent studies have shown that nanofluid (NF)-based minimum quantity lubrication (MQL) systems improved the machining lubrication and the titanium alloys' machinability. In this work, the tribological characteristics of a palm oil-based tripartite hybrid NF (ZnO/Al_2O_3/Graphene Oxide, GO) are studied. The novel usage of the developed lubricants in MQL systems was examined during the grinding of Ti6-Al-4V (TC4) alloy. The NF was produced by mixing three weight percent mixtures (i.e., 0.1, 0.5, and 1 wt.%) of the nanoparticles in palm oil. A comprehensive tribological and physical investigation was conducted on different percentage compositions of the developed NF to determine the optimum mix ratio of the lubricant. The findings indicate that increasing the NF concentration caused an increment in the dynamic viscosity and frictional coefficient of the NFs. The tripartite hybrid NF exhibited superior tribological and physicochemical properties compared with the pure palm and monotype-based NFs. Moreover, the dynamic viscosity of the tripartite-hybrid-based NFs increased by 12%, 5%, and 11.5% for the Al_2O_3, GO, and ZnO hybrid NFs, respectively. In addition, the machining results indicate that the tripartite hybrid NF lowered the surface roughness, specific grinding, grinding force ratio, tangential, and normal grinding forces by 42%, 40%, 16.5%, 41.5%, and 30%, respectively. Hence, the tripartite hybrid NFs remarkably enhanced the tribology and machining performance of the eco-friendly lubricant.

KEYWORDS hybrid nanolubricant, tribology, grinding, surface quality, Ti-6Al-4V, minimum quantity lubrication

1 Introduction

Machining processes are characterized by generation of an immense amount of heat around the contact zone. The traditional coolants prominent in the manufacturing industry have adverse environmental effects, produce greenhouse gasses, and are characterized by poor machining performances [1]. Moreover, during machining with traditional lubricants, the thermally induced surface and sub surface damages on the workpiece material increase [2]. The immense thermal energy generated during machining is the main cause of poor surface quality of the work material, which also reduces the life span of cutting tools. To decrease the adverse effects of greenhouse gases, campaigns toward the reduction of the amount of lubricants used in machining processes have been intense. Scientists have explained that a proper lubrication system that can effectively remove the heat from the contact zones can help decrease these unwanted machining problems. Hence, the utilization of the environmentally friendly cutting oils and

Received April 26, 2024; accepted June 15, 2024; online February 20, 2025

bio-enhanced nanolubricants has been promoted due to their enhanced tribological behaviors and eco-friendliness [3].

Ti-6Al-4V alloy (also referred to TC4) is a choice material for various advanced engineering applications due to its light weight, superior strength/toughness, high heat resistance, and corrosion resistance. TC4 is typically used in biomedical applications, maritime industries, and aerodynamic applications [4]. Similarly, TC4 alloys are classified under difficult-to-cut materials due to their low elastic modulus and heat conduction. Traditional lubricants often used during machining of TC4 alloys are expensive and cause several environmental and health hazards [5]. Hence, an alternate lubrication system for machining these materials must be found [6,7].

Minimum quality lubrication (MQL) involves spraying atomized oil droplets at high ejection pressure into the machining region. Studies have shown that the MQL system is a prime candidate for achieving this eco-friendliness in the machining of TC4 alloys [8–10]. Many researchers have reported that the use of MQL systems in machining these types of alloy materials can obtain improved surface quality, lower machining forces, and enhanced tool lifespan [11–13]. Several scientific reports have indicated that nanoenhanced lubricants possess higher thermal conductivity and excellent heat removal properties. Recently, the utilization of different nanoparticles (NPs) to produce bioenhanced lubricants for use in machining processes has increased. Previous research showed that water- or oil-based nano enhanced lubricants can effectively evacuate the heat generated in the contact zone [14].

Researchers have revealed that nanoenhanced biolubricants formed using multiple NPs exhibited superior tribological and thermophysical characteristics [15–18]. Hybrid nanoenhanced lubricants helped improve the machining performance in different processes such as turning [19,20], grinding [21–25], and milling [17,25,26]. Moreover, studies have indicated that hybrid nanofluids (NFs) increased the heat transfer characteristics in nanoenhanced lubricants [27]. Kalita et al. [28] reported that a hybrid NF containing MoS_2/Al_2O_3 when used in the MQL system produced better tribological performance compared with traditional lubrication techniques. Many researchers have used different combinations of NPs to form hybrid NFs. The composition and mixture solely depended on the properties of each NP and the corresponding physical characteristics that needed to be compensated for by each NP in the developed hybrid mixture.

Hybrid-based NFs have been studied extensively by many researchers. Examples include SWCNT/ZnO [29], Al_2O_3/ZnO [30], SiO_2/MWCNT [31], Al_2O_3/MWCNT [9]), Al_2O_3/SiO_2 [32], graphene/MWCNT [33], and Al_2O_3/GNP [34]. The findings from these works have indicated that hybrid NFs have superior thermophysical and tribological properties compared with the monotype/single NFs. Furthermore, despite the low heat conduction capacity of metal oxide-based NPs, they are favored for the producing NFs due to their low densities, higher oxidation resistances, and enhanced stability. Moreover, ZnO NPs is often selected for NF production due to its availability and low cost compared with other materials [35]. Lee et al. [36] and Mao et al. [37] explained the superb lubrication performance of oil- and water-based Al_2O_3 NFs in grinding operations, respectively. However, other researchers have shown that the lubrication performance of Al_2O_3 NF can be improved considerably by adding other types of oxide NPs to the fluid. Notably, NPs such as CuO, SiO_2, MWCNT, MoS_2, SiC, and graphene oxide (GO) have been used to improve the thermophysical and tribological properties of Al_2O_3-based NFs [23,32,38,39]. The thermal conductivity and lubricity of the hybrid NFs can be increased with a higher volume fraction of the NPs [40,41].

Mixed or hybrid NFs are now the main perspective for numerous researchers because they are currently thoroughly studied as potential alternatives to the traditional lubrication systems due to their superior antifriction capacity. Zhang et al. [42] explored the outcome of utilizing hybrid NFs in MQL systems for grinding Ni-based alloys. The evaluation was performed in terms of grinding forces, grinding force ratio, and surface roughness. The MoS_2/CNT mixed NPs achieved superior lubrication performance compared with the monotype NPs. Similar results were reported by authors [24,43]. Additionally, Hernández Battez al. [44] studied the rheological performance of hybrid NFs (i.e., MWCNT and TiO_2 NPs) manufactured with SAE50 oil. Compared with the pure base oil, the value of viscosity was lower in hybrid NFs at NF concentrations of less than 0.5 wt.%. However, the value of viscosity was higher when the NF concentration was raised from 0.5 to 1 wt.%.

Li [45] studied the tribological behavior of hybrid NPs (i.e., CeO_2 and TiO_2) with a combination ratio of 1:3. The concentration of 0.6 wt.% produced the best tribological performance. Moreover, Chu et al. [46] reported a substantial increase in thermal conductivity and dispersion capacity in MWCNT and Al_2O_3 water-based NF. Li et al. [47] conducted rheological analysis on different NF concentrations of hybrid lubricant (i.e., Acculube Lube2000 with graphene nanoplatelets/Al_2O_3). The hybrid NF could reduce the specific grinding energy by 91.78% and 80.25% compared with commercial lubricants and dry grinding, respectively.

Despite numerous investigations on the lubrication performances of hybrid NFs, work exploring the effect of tripartite-based hybrid NFs remain limited. Studies have shown that the thermophysical performance of multiple NPs mixed in a fluid can be considerably enhanced compared with those of the monotype-based NFs [16,17,48–50]. The use of multiple NPs to produce the

NF can compensate for deficient mechanical, physical, and tribological characteristics in the NF by the different NPs. Hence, an optimum NF combination and concentration for the tripartite-hybrid-based NF lubricants needs to be obtained. Previous works have indicated that the hybrid-based NF can be combined at a mixing ratio of 30:70 in the case of Al_2O_3-based NPs . Moreover, several other mix ratios have produced optimum lubrication performance. Apart from the mix composition, the NF's tribological characteristics depend on the shape, hardness, size, absorptiveness, hydrophilicity, and chemical interaction of each NP.

This work presents the production and novel uses of tripartite hybrid nanolubricant, which has been developed using GO, Al_2O_3, and ZnO NPs mixed in palm oil. The combination of these NPs was developed based on different explanations provided in previous kinds of literature. The NF was developed according to an initial hypothesis that explains how the individual NPs complement one another's tribological characteristics and enhance the tribology of the resultant NF. Similarly, studies have shown that these three NPs often employ the creation of slithering NF-based tribofilms for effective lubrication [51,52]. Preliminary rheological tests were performed on the manufactured lubricants to ascertain their tribological behaviors. Additionally, MQL-based grinding experiments were conducted to investigate the lubrication performance of the developed NFs. The grinding experiment was conducted on a TC4 workpiece material using a cubic boron nitride (CBN) grinding wheel. The lubrication performance from the grinding operations was evaluated based on the grinding forces, grinding force ratio, specific grinding energy, and surface quality. A graphical summary illustrating the structure of this work is presented in Fig. 1.

Figure 2 illustrates the flow and structure of this paper. This section explains the foundation laid by previous researchers on eco-friendly lubrication systems. Previous studies have established the mass exodus from using traditional lubrication systems in machining to using eco-friendly lubricants. Similarly, the recent utilization of NFs and MQL systems as lubricants is gaining more popularity due to their improved machining efficiency. Furthermore, with the advent of using multiple NPs in manufacturing NFs, previous works have shown that the hybrid NFs outperformed the monotype NF as lubricants in machining systems. This section also presents a brief overview of the recent investigations conducted on the grinding of Ti-6Al-4V alloy. Table 1 discusses the variables and results from different lubrication and grinding techniques utilized in machining the alloy material. Section 2 presents the material and methods employed and characterizes the NPs material and work material used. Section 2 also discusses the process involved in manufacturing the NFs, with extensive tribological investigations on the fluids. Section 3 details

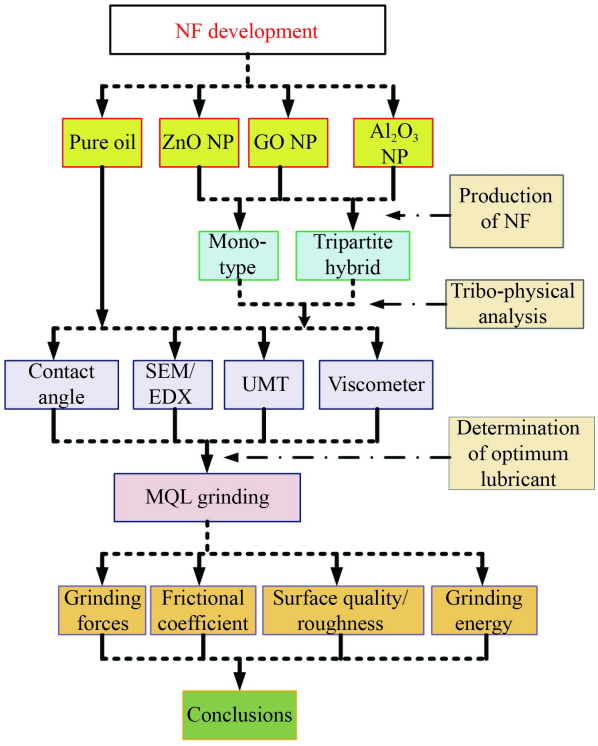

Fig. 1 Structure of the experimental study.

the grinding experiments conducted using the selected hybrid NFs. Section 4 reveals the results and notable observations from the experimental study. Section 5 presents a concise conclusion and an overall summary of the findings.

2 Materials and methods

In this section, the characterization of the NPs utilized for developing the NF is explained thoroughly. Similarly, the steps followed to develop the NFs/lubricants and the tribological/physical tests conducted on each of the lubricant are discussed succinctly. The two-step mixing technique was used to produce the NFs, and tribo-physical investigations were conducted through frictional and tribological tests.

2.1 Preparation of nanolubricants

The monotype- and tripartite-based NF samples were produced using different percentage weight concentrations of Al_2O_3, GO, and ZnO in a vegetable oil lubricant (Table 2 shows the physical properties). The NF concentrations considered included 0.1%, 0.5%, and 1%. Tables 2 and 3 present the process variables and the combination of variables considered to produce the NFs. Moreover, the average size of each NP was between 20 and 40 nm. Similarly, the dispersion behavior of the

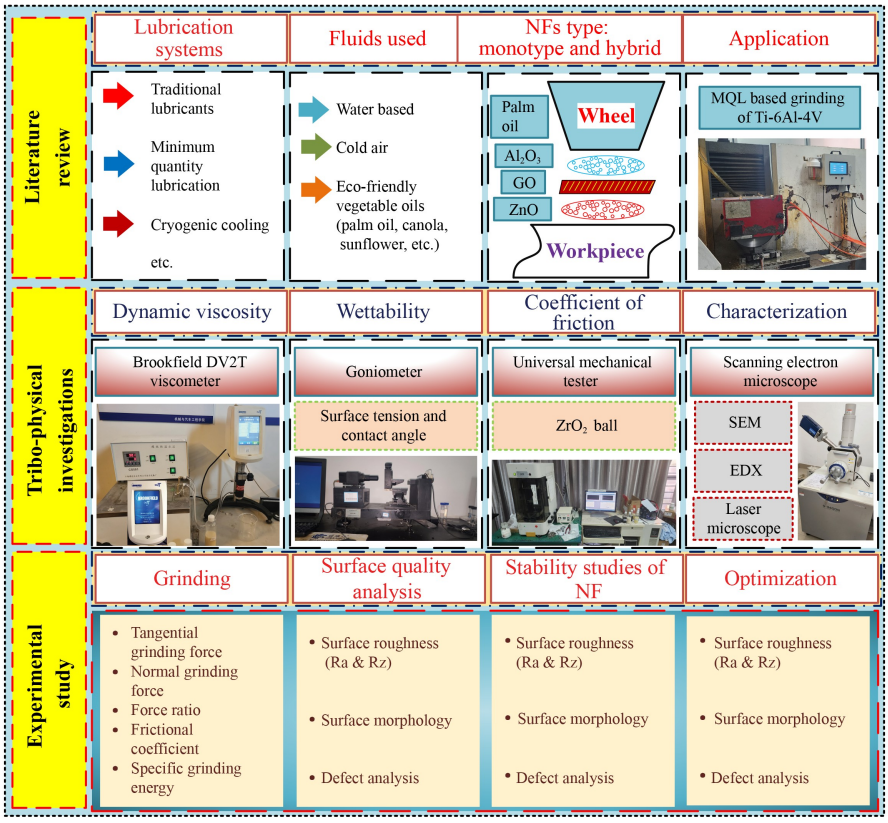

Fig. 2 Article structure.

lubricants on the workpiece surface was analyzed by measuring the contact angle of their droplets. This dispersibility behavior affects the thermal evacuation and lubricity of the lubricants. The contact angle was measured based on Young's contact angle formula, which provides the relation between the fluid, and surrounding air molecules [70]. The steps taken to produce the NF involved the two-step NF production technique, and an in-depth analysis of dynamic viscosity, friction behavior, and wettability of each lubricant followed. A schematic illustration of the preparation method and tribological tests conducted on the lubricants is shown in Fig. 3.

Palm-oil-based NFs were prepared by suspending the NPs in palm oil based on the total weight percentage of base oil, surfactant, and NP. The process variables and experimental run settings for manufacturing the NF are provided in Tables 3 and 4, respectively. The formula for weight percentage used in this work is shown in Eq. (1):

$$w_{\mathrm{nf}} = \frac{w_{\mathrm{np}} + w_{\mathrm{surf}}}{w_{\mathrm{np}} + w_{\mathrm{surf}} + w_{\mathrm{oil}}}, \tag{1}$$

where w_{nf} is the total weight percent of NF, w_{surf} is the total weight percent of surfactant and anti-oxidant, w_{np} is the total weight percent of individual NP, w_{oil} is the total weight percent of base oil (i.e., palm oil), and $w_{\mathrm{surf}} = 0.3w_{\mathrm{np}}$.

The resultant NF was then mixed using a magnetic stirrer for one hour to obtain a homogeneous mixture. Then, the produced NF was further mixed in an ultrasonic bath at a frequency of 40 kHz for another hour at room temperature to enhance dispersibility and prevent agglomeration. Previous studies have highlighted the importance of ultrasonication times on the stability and dispersibility of the NFs. Selecting an appropriate mixing period based on the properties of the individual NPs involved is vital because excessive sonication could lead to substantial physical and chemical deformations of the NPs [73–75]. Finally, a fully mixed homogenous NF was obtained. The NF samples were then kept at room temperature to observe the overall sedimentation of the fluid visibly.

2.2 Tribology testing of nanolubricants

The tribological experiments were conducted at atmospheric pressure at an approximate altitude of 67 m above sea level (Huangdao, Qingdao, China). The coefficient of friction (CoF) of each lubricant sample was obtained using a Brukers' universal mechanical tester (UMT) at the speed and load of 2 kHz and 20 N, respectively. The frictional tests were conducted on the UMT tribometer according to the standards of the American Society for Testing and Materials (ASTM) [52,76]. The tests were performed using a TC4 workpiece material of size 30 mm × 30 mm × 10 mm. The TC4 workpiece was polished to a mirror surface-finish (Ra =

Table 1 Literature review

S/N	Reference	System	Lubrication	NF concentration	Machining settings				Machining responses analyzed							
					v_s	v_w/(mm·min^{-1})	a_e/μm	f_u/kHz	f_t/N	f_n/N	Ra/μm	U/(J·mm^{-3})	μ	Grinding temperature/°C	V_b/μm	Σ/MPa
1	Singh H. et al. [53]	CG	MQL/canola oil	GNPs (1.5 wt.%)	22 m/min	3000	10	–	3.567	14.094	0.250	–	–	–	–	–
2	Mukhopadhyay and Kundu [54]	CG	RQL/blasocut water	–	14 m/min	–	10	–	26.92	58.53	0.64	–	0.6512	–	–	–
3	Guo and Yen [55]	CG	Flood	–	26.4 m/s	9	40	–	54	82	–	60	0.66	–	–	316.22
4	Rajeshkumar et al. [56]	CG	UMQL/sunflower oil	5 vol.%	20 m/s	6	10	–	26	70	0.5	–	–	–	–	–
5	Sadeghi et al. [57]	CG	MQL	–	15 m/s	20	7	–	34	38	025	–	–	–	–	–
6	Kacalak et al. [58]	CG	Flood	–	30 m/s	25	20	–	70	94	0.46	16	0.665	–	–	–
7	Abbas et al. [59]	Turning	MQL/ester oil	Al_2O_3 (4 vol.%)	32.1 m/s	111.6	25	–	–	–	0.515	–	–	–	1.65	–
8	Zhang et al. [60]	CG	Cryo-NMQL/ester oil	0.35%	4.02 m/min	1.12	15	–	52.37	–	–	62.84	–	183.9	–	–
9	Rajeshkumar et al. [56]	UAG	MQL/sunflower oil	1–10 vol.%	20 m/s	6	10	20	27	70	0.48	–	–	–	–	–
10	Kashyap et al. [27]	CG	MQL	–	22 m/s	3000	10	–	5.5	–	0.4	–	–	–	–	–
11	Ibrahim et al. [61]	CG	MQL/palm oil	GNP (0.1%–0.4%)	1800 r/min	4	10	–	10.24	50.3	0.278	24.12	0.21	–	–	–
12	Singh et al. [6]	CG	MQL/canola, olive, sunflower oils	GNO (1.5%)	22 m/s	3000	10	–	3.567	14.094	0.250	13	0.253	–	–	–
13	Wang et al. [62]	CG	MQL/palm oil	Al_2O_3 (2 wt.%)	30 m/s	3000	20	–	–	–	0.11	35.17	0.27	–	–	–
14	Dambatta et al. [63]	CG	MQL/canola	SiO_2 (0.2–6.5 wt.%)	32 m/s	1000	5	–	23	68	0.16	–	–	–	–	–
15	Seid Ahmed and González [64]	CG	MQL/palm oil	Graphene (0–0.1 wt.%)	30 m/s	1000	20	–	89	115	0.58	18.23	0.228	–	–	–
16	Zhang et al. [65]	CG	Cryo MQL	Al_2O_3 (0.35%)	15.2 m/s	4000	15	–	52.37	–	–	62.84	–	190	–	–
17	Lopes et al. [66]	CPG	MQL + CA	ITW Acculube 79053D	32 m/s	0.75	5	–	–	–	0.45	–	–	–	9	–
18	Cui et al. [8]	CG	Cryo MQL	Synthesized lipid	24 m/s	4000	10	–	46.8	61.4	0.468	–	–	151.2	–	–
19	de Moraes et al. [67]	CPG	MQL + CA	ITW Acculube 79053D	32 m/s	0.5	5	–	11	–	0.60	–	–	–	7	–
20	Zhang et al. [60]	CG	Cryo-NMQL	Synthesized lipid	24 m/s	4000	10	–	–	–	0.375	51.96	0.6	155.9	–	–
21	Mukhopadhyay and Kundu [54]	CG	SQL/MQL	Propylene glycol, sodium nitrite, soap water, blasocut	30.17 m/s	1400	15	–	23	55	1.5	38	0.6	–	–	–
22	Liu et al. [68]	CG	Cryo MQL	Plant-based F 30A	30 m/s	4000	30	–	48.6	51	0.42	42.66	0.32	232.1	–	–
23	Dambatta et al. [69]	UAG	MQL/canola, corn, sunflower	SiO_2	31.42 m/s	1000	10	20	29.4	65	0.456	55.43	0.4519	–	–	–

10 nm) using a Technipol PRO VS rotary polisher. The TC4 flat sample moved in reciprocating form with a sliding speed of 0.1 m/s and stroke of 6 mm for 20 min. A G5 precision-grade zirconia ball with a diameter of 9.5 mm was kept fixed and subjected to a normal load of 20 N. Before conducting each frictional test, the test samples were thoroughly eviscerated using acetone to remove any dirt. To ensure improved accuracy of the results, the experiment for frictional coefficients was repeated thrice, and the average values were recorded.

Table 2 Characteristics of NPs [71,72]

S/N	Properties	Unit	Al_2O_3	GO	ZnO
1	Specific heat	J/(kg·K)	880	710	501
2	Thermal expansion coefficient	10^{-6}/°C	8.1	−67	6.5
3	Melting point	°C	2055	3600	2248
4	Density	kg/m^3	3600	1800	5606
5	Thermal conductivity at 330 K	W/(m·K)	36	18	50
6	Hardness	Mohs	9	–	5
7	Compressive strength	MPa	62.4	76	67
8	Young's modulus	GPa	215	230	140
9	Fracture toughness	MPa·m$^{1/2}$	3.5	6.7	2.44
10	Color	–	White	Black	White

2.3 Viscosity

The dynamic viscosity of the pure palm oil and palm-oil-based NFs was measured using a Brookfield viscometer at shear rates of 50 s^{-1}. The dynamic viscosity of each fluid was determined using a rotating UL adapter. The experiment for the dynamic viscosity in each fluid was performed thrice, and the average readings were recorded. The dynamic viscosity was measured at temperatures of

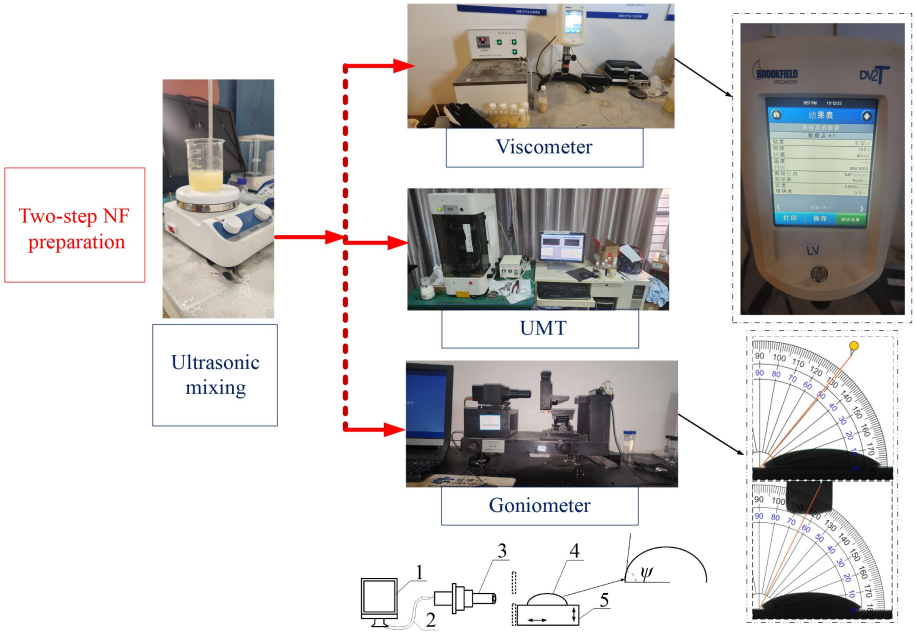

Fig. 3 Illustration of the NF preparation and tribological investigations (coefficient of friction, dynamic viscosity, and contact angle ψ). 1. Computer; 2. Connectors; 3. Microscopic lens; 4. Fluid droplet; 5. Moveable lever.

Table 3 Process parameters

S/N	Mode	NF concentration/wt.%	Composition
1	Monotype NP	0	100% Al_2O_3
2	Al_2O_3 based	0.1	100% ZnO
3	GO based	0.5	100% GO
4	ZnO based	1.0	50%:10%:40% (Al_2O_3/ZnO/GO)
5	–	–	50%:40%:10% (Al_2O_3/ZnO/GO)
6	–	–	50%:10%:40% (GO/Al_2O_3/ZnO)
7	–	–	50%:40%:10% (GO/Al_2O_3/ZnO)
8	–	–	50%:10%:40% (ZnOAl_2O_3/GO)
9	–	–	50%:40%:10% (ZnO/Al_2O_3/GO)

Table 4 Settings for experimental runs

Sample No.		NF concentration/wt.%	Composition
1	–	0.1	Al_2O_3
2	–	0.1	GO
3	–	0.1	ZnO
4	–	0.5	Al_2O_3
5	–	0.5	GO
6	–	0.5	ZnO
7	–	1.0	Al_2O_3
8	–	1.0	GO
9	–	1.0	ZnO
10	Al_2O_3 based	0.1	50% Al_2O_3 + 40% ZnO + 10% GO
11		0.1	50% Al_2O_3 + 40% GO + 10% ZnO
12		0.5	50% Al_2O_3 + 40% ZnO + 10% GO
13		0.5	50% Al_2O_3 + 40% GO + 10% ZnO
14		1.0	50% Al_2O_3 + 40% ZnO + 10% GO
15		1.0	50% Al_2O_3 + 40% GO + 10% ZnO
16	GO based	0.1	50% GO + 40% ZnO + 10% Al_2O_3
17		0.1	50% GO + 40% Al_2O_3 + 10% ZnO
18		0.5	50% GO + 40% ZnO + 10% Al_2O_3
19		0.5	50% GO + 40% Al_2O_3 + 10% ZnO
20		1.0	50% GO + 40% ZnO + 10% Al_2O_3
21		1.0	50% GO + 40% Al_2O_3 + 10% ZnO
22	ZnO based	0.1	50% ZnO + 40% GO + 10% Al_2O_3
23		0.1	50% ZnO + 40% Al_2O_3 + 10% GO
24		0.5	50% ZnO + 40% GO + 10% Al_2O_3
25		0.5	50% ZnO + 40% Al_2O_3 + 10% GO
26		1.0	50% ZnO + 40% GO + 10% Al_2O_3
27		1.0	50% ZnO + 40% Al_2O_3 + 10% GO
28	–	Pure palm MQL	–

30, 50, 75, and 90 °C. Pure palm oil exhibited the lowest dynamic viscosity among all the measured lubricants across different temperatures. Similarly, the hybrid NFs had higher dynamic viscosities than the monotype ones. The dynamic viscosity of the NF improved substantially as the NF concentration increased. In the tripartite-based NF samples, the ZnO and Al_2O_3 NPs had a higher effect on the dynamic viscosity than the GO NPs. However, at higher measurement temperatures, the dynamic viscosities across all the NFs were similar. Consequently, the overall values of the dynamic in all the NFs reduced drastically as the temperature increased.

2.3.1 Theoretical model for viscosity of hybrid NFs

Many theoretical models have been developed for calculating the viscosity of fluids. The earliest were presented based on the volume concentration of particles and the fluid. Hence, the volume concentration of the NF (Ψ_{nf}) in Eq. (2) can be obtained by modifying Eq. (1).

$$\Psi_{nf} = \frac{\dfrac{w_{np}}{\rho_{NPs}} + \dfrac{w_{surf}}{\rho_{surf}}}{\dfrac{w_{NPs}}{\rho_{NPs}} + \dfrac{w_{surf}}{\rho_{surf}} + \dfrac{w_{oil}}{\rho_{oil}}} \times 100\%. \quad (2)$$

Einstein [77] presented the viscosity formula of a fluid according to the particles present in the fluid. The model deliberated on "small rigid spheres suspended in a liquid". Several studies have been done to compute the dynamic viscosity of NFs through physical, thermodynamic, and nonrheological variables. The models developed often neglected the effect of different rheological variables on the viscosity of the fluid. Further, the Einstein theoretical model for viscosity calculation (Eq. (3) [77]) was only accurate for fluids with concentration below 0.0245 vol.%. Likewise, Einstein's equation did not account for the behavior of the hybrid or multiple particles present inside the base fluid. Over the

years, many modifications have been made to the viscosity equation due to the discovery of NPs of different shapes.

$$\frac{\mu_{nf}}{\mu_{bf}} = 1 + 2.5\Psi, \tag{3}$$

where μ_{bf} is base fluid's viscosity, and $\Psi < 0.0245$ is the volumetric fraction.

Batchelor [78] modified Einstein's equation to consider the Brownian motion and entropy within the fluid and arrived at Eq. (4):

$$\frac{\mu_{nf}}{\mu_{bf}} = 1 + 2.5\Psi + 6.5\Psi^2. \tag{4}$$

Furthermore, upon the discovery of NPs, Masoumi et al. [79] modified the theoretical models. The Masoumi model is shown in the following equation [30,79]:

$$\frac{\mu_{nf}}{\mu_{bf}} = 1 + 2.5\Psi + \frac{\rho_p + V_B + d_p^2}{72 \cdot \delta \cdot C_f}, \tag{5}$$

where V_B is the Brownian velocity of particles, ρ_p is the density of NP, d_p is the diameter of NPs, C_f is the correlation factor, and δ is the average distance between the NPs.

Moreover, the factors V_B, C_f, and δ may be simplified into Eqs. (6)–(8), respectively.

$$V_B = \left(\frac{18RT}{\pi N_A \rho_p d_p^3}\right)^{1/2}, \tag{6}$$

$$C_f = \frac{10^{-10} \cdot T \cdot \Psi^{-0.002T-0.284}}{\mu_{bf}}, \tag{7}$$

$$\delta = \left(\frac{\pi d_p^3}{6\Psi}\right)^{1/3}, \tag{8}$$

where R is the gas constant, t is the temperature, and N_A is the Avogadro's number [79].

Udawattha et al. [80] presented the recent improvements to the Masoumi equation considering the weight of multiple NPs present in the fluid. Equation (9) indicates the theoretical model of the viscosity of hybrid NFs presented by Udawattha et al. [80].

$$\frac{\mu_{nf}}{\mu_{bf}} = 1 + 2.5\sum_{i=1}^{n_{NPs}} \Psi_{Ei} + \sum_{i=1}^{n_{NPs}} \mu_{dyi}, \tag{9}$$

where n_{NPs} is the number of NPs and Ψ_{Ei} is the volume concentration of NPs.

Therefore, the viscosity of the NF depends on the density of the NPs and the distance between the particles in the fluid [30]:

$$\sum_{i=1}^{n} \mu_{dyi} = \frac{\rho_{pi} + V_{Bi} + d_{pi}^2}{72 \cdot \delta_i \cdot C_f}. \tag{10}$$

The improved Udawattha model encompasses the parameters neglected by the earlier models; hence, it is regarded to be more precise. The improved Udawattha model considers the density of individual NPs and their distance apart. Likewise, recent studies have shown that the utilization of statistical and intelligent-based techniques built on existing theoretical models can be used to predict the viscosity of NFs with greater accuracy [30,81]. However, in recent peculiar cases with multiple NPs (hybrid) present in a mixture of two or more base fluids [54], the density component of Eq. (2) then includes the individual density of each fluid present.

Theoretical models of calculating the dynamic viscosity of an NF often relate to the mixing enthalpy and activation energy of the fluid mixture. Moreover, few research works have focused on the effect of the shapes of multiple NPs on the dynamic viscosity of the NF [82]. Hence, using the improved Einstein's equation by Kondratiev and Jak [83], Eq. (3) can be modified into Eq. (12). Likewise, the viscosity of the NF can be obtained by considering the concentration of the NF, by further modifying Eq. (12) [83] into Eq. (13).

$$\frac{\mu_{nf}}{\mu_{bf}} = (1 - \bar{R}\Psi)^{-n}, \Psi < 0.0245, \tag{11}$$

$$\mu = \mu_{bf}(1 - \alpha\Psi)^{-n}, \tag{12}$$

where $\bar{R}$ and n are predetermined variables. $\bar{R}$ is 1.35 for similar-shaped NPs and 2.5 for dissimilar-shaped NPs. n is 1.0 for particles with the same shape/size and 2.5 for dissimilar-shaped particles. α = transpose of the coefficient of solid phases [84].

2.4 Wetness ability

The wetness ability of a lubricant is an important property that affects the overall grinding performance of MQL [22]. Hence, the wetness ability of each lubricant must be determined. The wetness ability, often referred to as wettability, can be determined by analyzing the contact angle ψ of the lubricant droplet on the surface of the titanium alloy [52,85].

Previous researchers have indicated a direct relation between the surface tension and the contact angles of a lubricant. Li et al. [86] explained the mathematical relationship between the contact angle and the surface tensions on a fluid droplet where they related the contact angle with the surface tension as $\cos\psi = (\tau_{ac} - \tau_{ab})/\tau_{bc}$. A higher surface tension led to an increase in the contact angle and the area covered by the droplet [87]. Figure 4 illustrates the method used to measure the contact angles of each lubricant sample using a dropping of the fluid on the surface of the TC4 alloy. The contact angle of each lubricant sample was measured, and the image of the oil droplet was obtained according to ASTM D7334-08 standards [88]. The contact angles of each lubricant sample was measured using a 2009JC120 Powereach goniometer manufactured by Shanghai Zhongchen Digital Technology Apparatus Company. The average contact angle was obtained for each lubricant sample after

three measurements, and the work material was cleaned thoroughly using acetone before each experiment.

2.5 Characterization of materials

The composition of each NP was obtained using a Hitachi S-3400N scanning electron microscope (SEM). Before the SEM analysis, the surface of each sample was prepared with Au particles in a DC magnetic sputtering machine at 10 Pa and 10 mA DC for 60 s. Figures 5(a)–5(c) show the SEM images with the elemental compositions of the Al_2O_3, GO, and ZnO NPs, respectively. The spectrum analysis shows the existence of the identified elements through their atomic weights. The ZnO and Al_2O_3 NPs were round and spherical, whereas the GO were flat and flake-like.

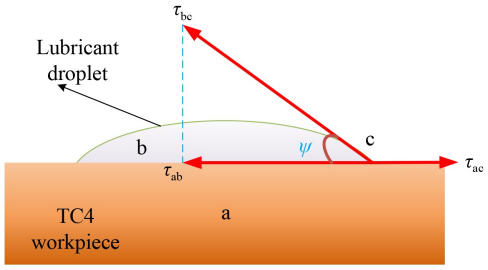

Fig. 4 Illustration of measurements of surface tension and contact angle of a fluid droplet.

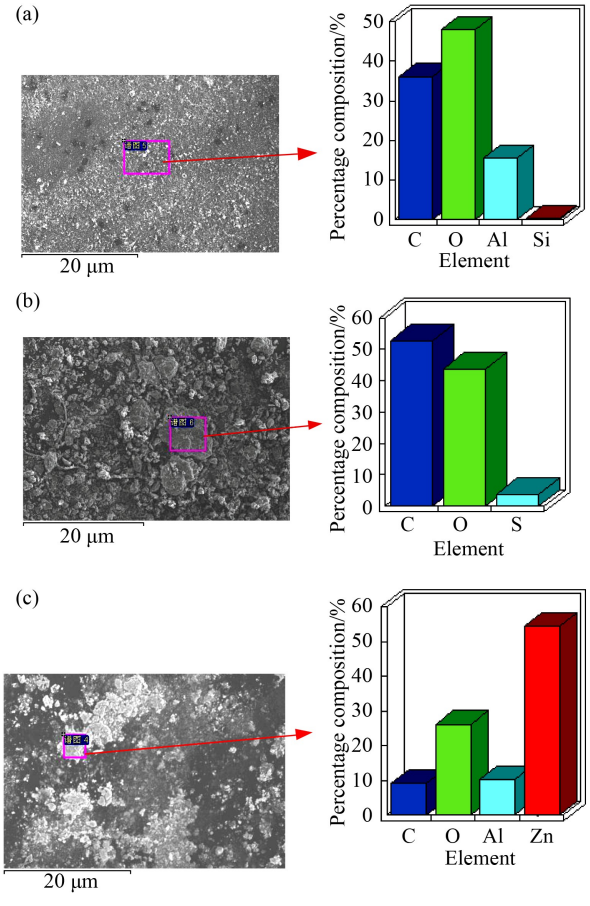

Fig. 5 SEM and EDX compositions of NPs: (a) Al_2O_3, (b) GO, and (c) ZnO.

3 Grinding experimentation

This section fully explains the grinding experiments conducted on the TC4 alloy using the optimal NF concentration. The experimental design was developed to provide a basis for comparison between the tripartite-hybrid-based NF and the other lubricants.

The machining was performed on a model K-P36 grinding machine using a CBN grinding wheel. The dimension of the CBN grinding wheel was 300 mm × 20 mm × 76.2 mm. Additionally, the ejection pressure and fluid flow rate of the MQL system were set as 0.35 MPa and 100 mL/h, respectively. To enhance fluid delivery, the settings for nozzle distance from the contact zone and its angle of inclination were selected based on optimized values of authors [6,42,54,89]. The grinding experiments were then performed to assess the overall performance of the palm-oil-based NFs. The experimental runs were repeated thrice, and the average values of each response was recorded. Furthermore, the grinding wheel was fully dressed before each experimental run. The grinding operations were done on a 40 mm × 30 mm × 30 mm TC4 alloy material (i.e., TC4 with composition of Ti-89.5%, Al-6.12%, V-3.74%, Fe-0.3%, and others-0.34%). The physical and mechanical properties of the titanium alloy are presented in Table 5.

The grinding operations were conducted using the MQL system with pure and hybrid palm-oil-based NFs with the machine settings presented in Table 6. Furthermore, the grinding forces (i.e., tangential and normal) were obtained with the help of a YDM-III99 dynamometer. The setup of the grinding machine and MQL system are shown in Fig. 6. The magnitude of multiaxial grinding forces generated during each grinding pass was recorded from the dynamometer at a sampling frequency of 1 kHz over 3401 cycles. A Zishu USB3214 multifunctional voltage data acquisition card, which was

Table 5 Physical properties of the TC4 alloy material

S/N	Physical property	Value	Unit
1	Thermal conductivity	7.955	W/(m·K)
2	Specific heat	526.3	J/(Kg·K)
3	Density	4.42	kg/m^3
4	Modulus of Elasticity	114	GPa
5	Poisson's ratio	0.342	–
6	Shearing strength	700	MPa
7	Hardness	35	GPa (Rockwell)
8	Yield strength	880	MPa

connected to a digital/analog analyzer (DAQ-Explorer), was then used to analyze the output from the YDM-III99 dynamometer.

Moreover, the surface quality of the workpiece material was measured quantitatively using surface roughness, whereas qualitative analysis was conducted using SEM. The ground sample material was properly cleaned in an alcohol bath to remove grinding debris and dirt. Then, the surface quality, roughness (surface roughness Ra and another roughness component Rz), and texture of the ground samples were acquired using a 20 × magnification in an Olympus laser microscope (OLS5000). Furthermore, to optimize the energy consumption during machining, the performance of each lubricant sample was assessed using the specific grinding energy and CoF obtained from Eqs. (14) and (15), respectively.

$$U = \frac{v_s f_t}{a_e v_w b}, \tag{13}$$

$$\mu = \frac{f_t}{f_n}, \tag{14}$$

Table 6 Parameter settings of grinding operation

S/N	Parameter	Symbol	Value	Unit
1	Grinding depth	a_e	10	μm
2	Wheel speed	v_s	31	m/s
3	Table feed	v_w	1000	mm/min
4	MQL nozzle angle of inclination	α	22	°
5	MQL ejection distance	d	20	mm
6	Droplets flow rate	Q_m	80	mL/h
7	Ejection pressure	P	0.35	MPa

where f_t is the tangential grinding force, f_n is the normal grinding force, v_w is the feed rate, v_s is the wheel speed, b is the wheel width, and a_e is the grinding depth.

4 Results and discussion

This section presents the results and discussion of the experiments in the preceding sections. First, the stability of the NFs was studied using the visual analysis technique. Similarly, the tribological performance of each lubricant was evaluated using the frictional tests and measurement of dynamic viscosity. Moreover, the wettability of the NFs was analyzed, and the best lubricant sample was acquired. Lastly, the grinding performance of the NFs was examined based on the grinding forces and final surface topography of the ground TC4 alloy.

4.1 Analysis of the nanolubricant performance

4.1.1 Visual observation samples

The NF samples were studied over regular time intervals, and their settling processes were carefully observed. The settling was visually assessed at regular intervals, and the image after each study period was captured. Previous researchers used the visual assessment process, which confirmed it to be a viable technique for assessing the stability of NFs [90,91]. In addition, the dispersive stability of the hybrid NFs was evaluated over some time. The fluids were placed unagitated at room temperature

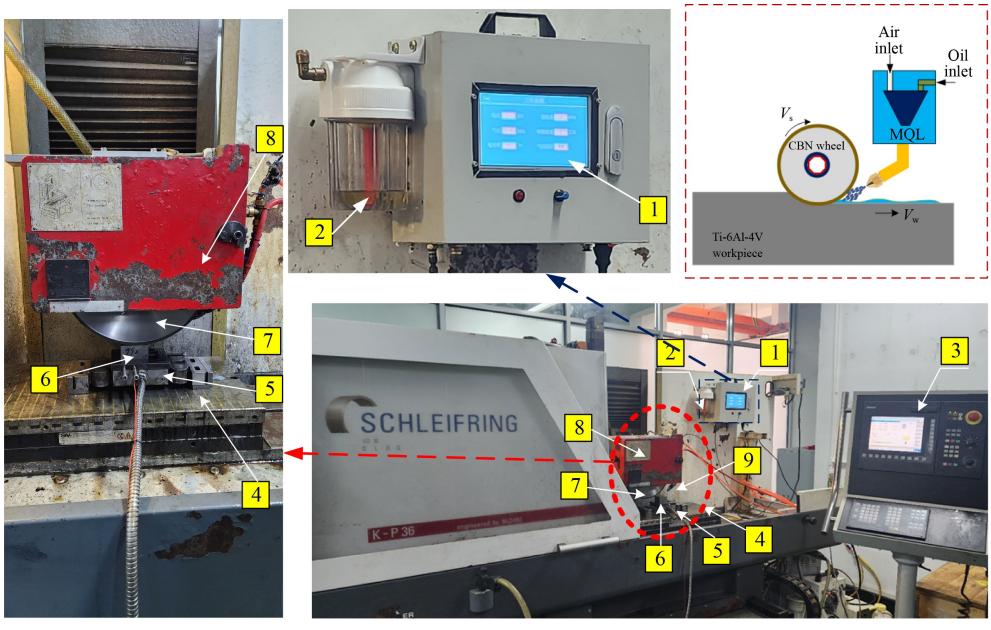

Fig. 6 Grinding machine and MQL set-up. 1. MQL system; 2. MQL fluid tank; 3. CNC control panel; 4. Magnetic table; 5. Dynamometer; 6. TC4 workpiece; 7. CBN grinding wheel; 8. Hydraulic control; 9. MQL nozzle.

until the total time needed for complete agglomeration at the bottom was attained. The images in Fig. 7 show the state of the manufactured NF studied for 36 days. The agglomeration of the NFs was noticeable within 14 days of ultrasonic mixing. Moreover, the NFs exhibited settling times. In the monotype NFs, the ZnO NF settled faster than the Al_2O_3 and GO-based NFs. Furthermore, the concentrations of 0.1 and 0.5 wt.% attained full sedimentation in 12 days, whereas the 1 wt.% attained full sedimentation after 21 days. In addition, Fig. 7 shows that the GO and Al_2O_3 monotype NF at 1% concentration had the highest settling times. Moreover, the monotype Al_2O_3 and GO NF at 1% NF concentration exhibited enhanced tribological characteristics compared with the ZnO-based NF. However the tribological properties of the monotype NF were lower than those of the tripartite-hybrid-based NFs. Further, the 1% concentration tripartite hybrid NFs had a superior stability compared with the monotype ones. The results ascertained that the monotype ZnO NF settled faster than the Al_2O_3- and GO-based NFs. Additionally, the concentrations of 0.1 and 0.5 wt.% attained full sedimentation within 300 h, whereas the 1 wt.% concentration achieved sedimentation in about 21 d.

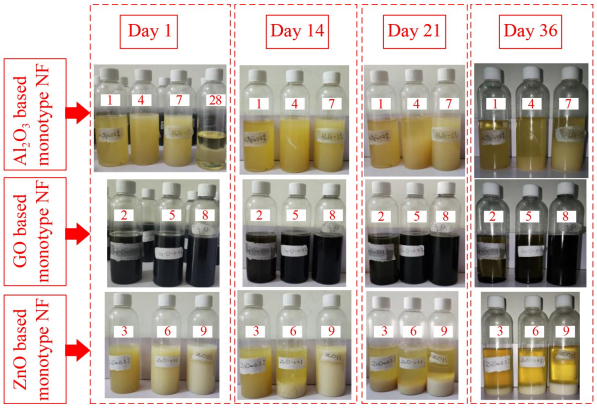

Fig. 7 Images of monotype NF visual stability analysis.

The tripartite hybrid NFs at 1% concentration had the longest settling times compared with pure palm oil, 0.1%, and 0.5% concentration NFs (Fig. 8). The tripartite hybrid NF concentrations of 1 wt.% demonstrated superior dispersibility and stability. Moreover, as shown in Fig. 8 for the tripartite hybrid based NFs, the samples with smaller percentages of GO NPs exhibited superior suspension capacity. This outcome could be attributed to the higher surface adsorption energy and the resultant effect of gravity on the GO NPs. For instance, sample No. 14 had only 10% of GO, which was lower than the 40% sample number 15, and the former exhibited faster sedimentation. Similar observations were made across all the samples produced using 40% or higher weight percentage of GO NPs.

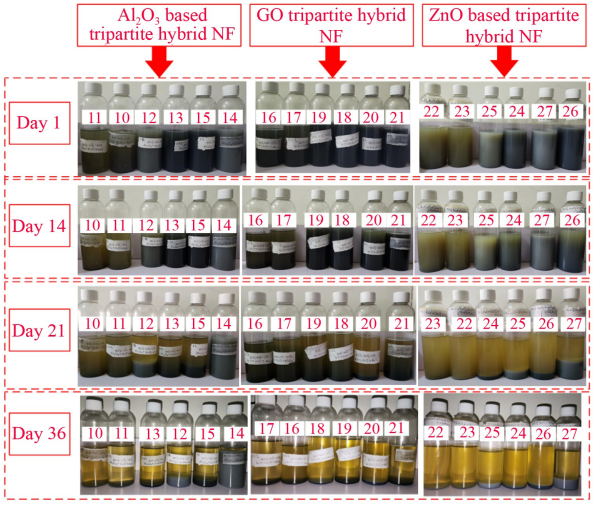

Fig. 8 Images of tripartite hybrid based NF visual stability analysis.

In addition, the tripartite hybrid Al_2O_3-based NF had the longest settling time. In the case of the GO tripartite hybrid NPs, the NF contained a high amount of black deposits spread at the bottom of the mixture in the first five days of production. Additionally, the effect of the surfactant was more apparent in the 1% concentration tripartite hybrid based NFs due to the higher amount of the surfactant used. This increase in the amount of the surfactant and antioxidant supplement in the 1% concentration samples could explain its improved miscibility and stability.

Lastly, a notable observation was seen in the GO-based NFs of sample No. 21 after two months of producing the lubricants. The NF condensed due to thorough mixing and interaction of the GO and Al_2O_3 NPs, and formed a sludge-like and highly viscous liquid.

The performance of the nanolubricants manufactured through suspension of different weights of the NP in the based oil was further analyzed. The experimental results indicated a resultant increase in tribological performance by increasing the concentration of NP from 0% to 1%. Generally, the contact angles of NF were higher than those of pure oil. The Al_2O_3- and ZnO-based NFs presented similar tribological results, which were better than the GO NF. Similar results were observed for the other responses, namely, dynamic viscosity, wear, and CoF. Moreover, the tripartite hybrid NF (i.e., Al_2O_3/GO/ZnO) showed improved results compared with the monotype NFs. The highest values for each response parameter were recorded when the NF concentration was 1 wt.%. This outcome agreed with the findings of previous researchers who stated that the 1% NF concentration for hybrid/dual NPs produced optimal tribological behaviors [70,92,93]. The findings indicated that the addition of NPs to pure palm oil helped increase the spritz area of the manufactured fluid. Regarding the dynamic viscosity, the monotype GO NF illustrated

enhanced thermophysical behavior compared with the Al_2O_3 and ZnO NFs. However, the tripartite hybrid NF exhibited the best thermal behavior, which also increased with higher NF concentrations. This outcome was evident from the results of dynamic viscosity obtained at elevated temperatures. However, the dynamic viscosities of the mono and tripartite hybrid NFs at the extreme temperature of 90 °C were similar for all NFs. Regarding the contact angle, the addition of NPs into the palm oil produced higher spreading and contact angle of the resultant NF samples. The NF with a higher proportion of alumina and ZnO NP presented the highest contact angle compared with the other tripartite hybrid and mono NF samples.

4.1.2 Coefficient of friction

The total amount of energy consumed during the grinding operations largely depends on the CoF existing between the various chaffing components, that is, the grinding wheel and the work material. The amount of energy expended in grinding can be reduced considerably by appropriate lubrication and grinding conditions. Nonetheless, the complex interaction in the contact region involves multiple force types, and the impetuous hammering actions of the wheel grits on the work material produce a tremendous amount of grinding-induced damage. Hence, obtaining an effective lubrication that can substantially decrease the frictional coefficient is essential. Tribological investigation on the UMT machine is one of the ways to determine the frictional coefficient of a lubricant by the continuous chafing actions [61,94]. The operation of the Bruckers UMT is equivalent to scaling down the grinding to the operation of a single grit. The frictional behavior of a lubricant can be studied on the UMT machine because its operation imitates continuous scratching, similar to what exists in the grinding process's contact zone.

After the tribological analysis of each lubricant on the UMT machine, the final topography of the ZrO_2 ball and TC4 workpiece was analyzed using the Olympus OLS5000 laser microscope. Figure 9 shows that the

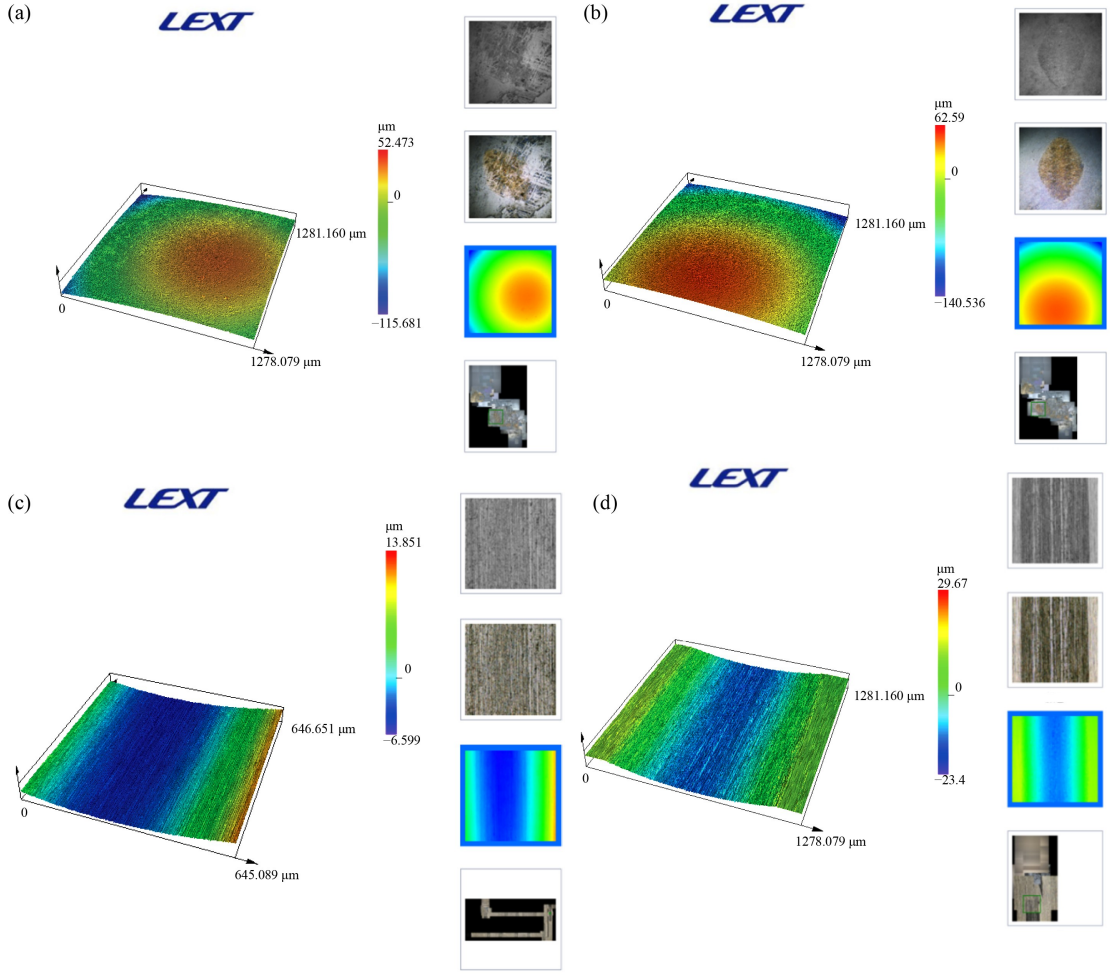

Fig. 9 Topography of samples from frictional/tribological tests: (a) ZrO_2 ball from sample 5, (b) ZrO_2 ball from sample 20, (c) scratched TC4 from sample 5, and (d) scratched TC4 from sample 20.

surface quality of the ball and the work material differed and were highly dependent on the lubricity of the lubricant utilized. The surface texture of the rubbed surfaces from oil samples 5 and 20 were used to illustrate the effect of frictional coefficient on the surface quality of the components. The results showed a remarkable difference between the topography of ground parts using monotype and hybrid tripartite NF.

Figure 10 reveals the results of CoF for the different lubricants obtained by rubbing the ZrO_2 ball and the titanium alloy material. The highest CoF was recorded when pure palm oil was used as the lubricant. The average CoF values for the pure palm oil at 15 and 600 s were 0.425 and 0.326, respectively. However, the CoF was reduced considerably when NF concentration was increased (Fig. 10). CoF drastically reduced between times 20 to 120 s. Beyond the 300 s mark, the magnitude of CoF obtained in each sample was not considerably different.

Figure 11 shows that the performance of each lubricant sample corresponded to the properties of the dominant NP in the fluid. Regarding the tripartite-hybrid-based NF, multiple NPs helped considerably improve the CoF, and the lowest and highest CoFs were obtained in the 1% and

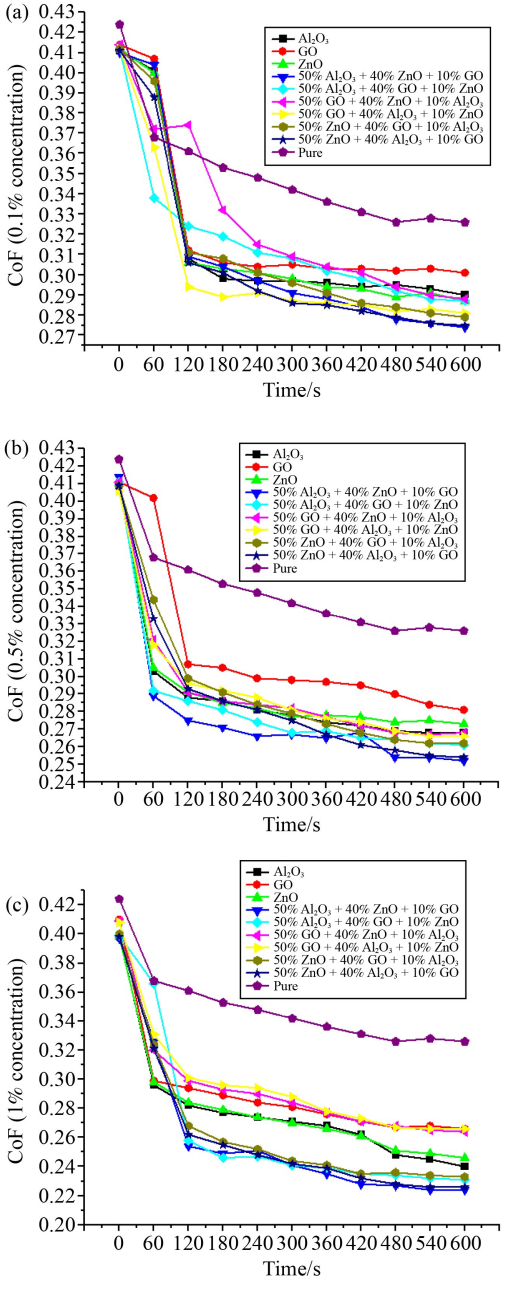

Fig. 10 Influence of NF concentration on CoF: (a) 0.1%, (b) 0.5%, and (c) 1%.

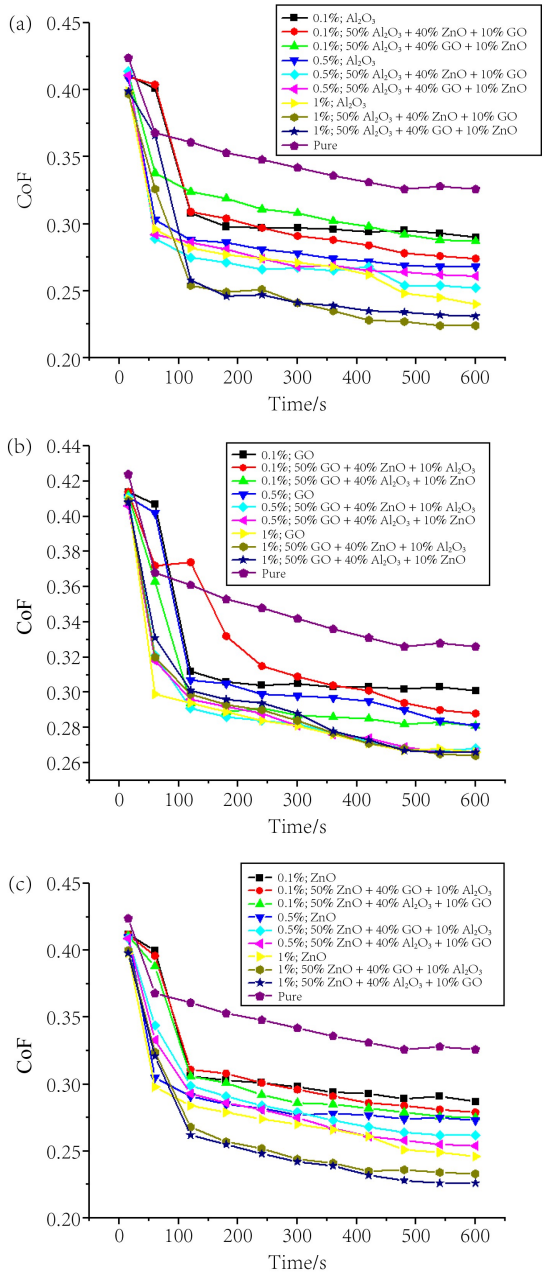

Fig. 11 Influence of nanoparticle types on CoF: (a) Al_2O_3 based, (b) GO based, and (c) ZnO based.

0.1% NF concentration samples, respectively. The CoF can be increased by increasing the NF concentration. Although previous works have shown that the CoF decreases when the NF concentration was increased from 0% to 0.1% [61], our findings indicate a steady increase of the CoF as the NF concentration was increased from low to high concentrations (i.e., 0%, 0.1%, 0.5%, and 1%). Likewise, the 1% concentration of Al_2O_3-based tripartite hybrid NF (sample 14) exhibited the lowest CoF (0.226 μm) after 600 s of the analysis. A closely related result was obtained in the 1% concentration of ZnO-based tripartite hybrid NF (sample 27).

In addition, the results obtained from the tribological testing confirmed that the individual NPs exhibited different mechanical behavior when subjected to intense shearing stress. Nevertheless, the GO-based NFs delaminated after about 120 s of shearing action in the UMT machine. This outcome could be attributed to the frail structural bonding existing in the GO NPs. The delamination of the GO NP may seem like a setback in its tribological behavior, but it facilitated the lubricity of the GO-based NF during the rubbing operations. This finding corroborated the explanations of previous authors [70,95]. Moreover, the synergistic interaction between the three oxide-based NPs remarkably improved the dynamic viscosity of the tripartite hybrid NFs, especially at higher NF concentrations. Finally, the CoF of the tripartite hybrid based NFs was higher than those of the monotype NFs and pure palm oil.

4.1.3 Dynamic viscosity

The dynamic viscosity of a fluid measures its resistance to steady mechanical motion. Because the viscosity of NFs depends on several variables, the NFs can exhibit Newtonian and non-Newtonian characteristics. Hence, the results obtained in this work show that the tripartite hybrid based NF exhibited the characteristics of a Newtonian fluid as the temperature was increased from 30 to 90 °C. Figure 12 visually compares the different results for the dynamic viscosity of each lubricant sample at several temperatures based on the dominant NPs in the fluid. In each lubricant sample, an increase in the temperature caused a lower value of the dynamic viscosity (i.e., inverse relation). This phenomenon can be explained by the behavior of the fluid from the basic principles of physics. The rising temperature caused higher entropy and energy state of the individual atoms and thereby increased the spacing between the NP and the palm oil.

The results of dynamic viscosity showed that compared with the smaller NF concentrations, the 1% NF concentration presented a higher dynamic viscosity at elevated temperature of 90 °C. Additionally, critically analyzing the performances of the monotype NFs

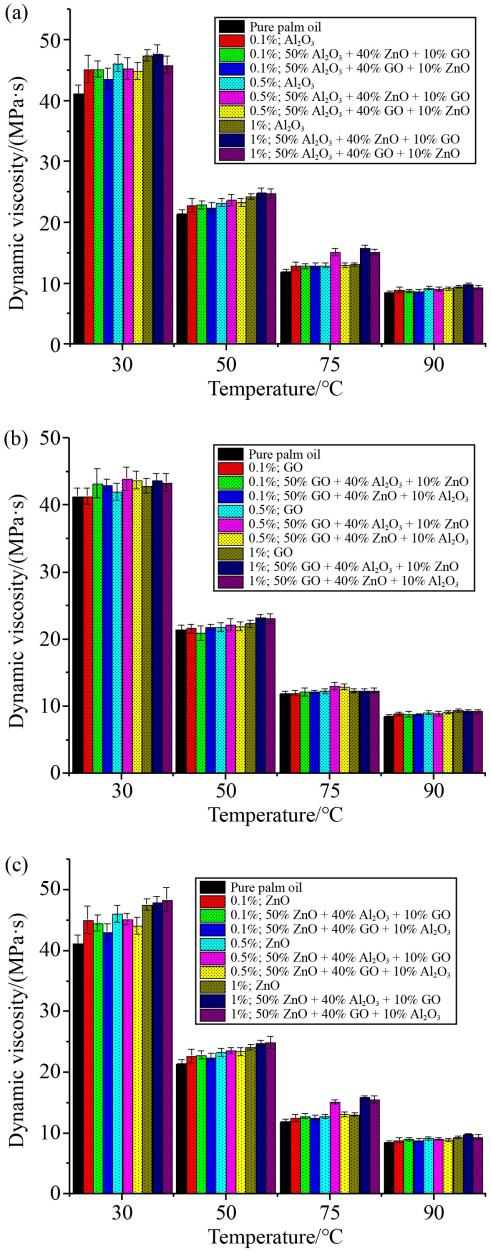

Fig. 12 Influence of different NF types on dynamic viscosity: (a) Al_2O_3 based, (b) GO based, and (c) ZnO based.

indicated that the Al_2O_3 based NF presented a superior thermophysical behavior compared with the GO and ZnO NPs. This outcome is evident from the higher values of dynamic viscosity measured in the monotype-based Al_2O_3 NFs. Furthermore, the best-performing samples in terms of dynamic viscosity from the experimental study were the tripartite hybrid NF from samples 14 and 27. Samples 14 and 27 exhibited similar thermodynamic responses. Figure 12(a) illustrates the result of the dynamic viscosity of the Al_2O_3-based lubricants at different temperatures. Dynamic viscosity was directly proportional to NF concentration but inversely related to temperature. Likewise, Fig. 12(b) presents the result of

the dynamic viscosity of the GO-based NFs. The tripartite hybrid NF from sample No. 23 with composition (50% GO:40% Al_2O_3:10% ZnO) produced the best results for the dynamic viscosity measured at different temperatures. Moreover, at high temperatures, the difference in magnitude of the dynamic viscosity between the 0.5% and 1% concentration NFs was not evident. Equally, in Fig. 12(c), the tripartite hybrid NF of sample No. 27 with a mix-proportion of 50% ZnO + 40% Al_2O_3 + 10% GO presented the best results of dynamic viscosity among all the ZnO-based NF samples.

Figure 13 presents a graphical comparison of the dynamic viscosity based on the NF concentrations. The 1% NF concentration exhibited the highest magnitude of dynamic viscosity at high and low temperatures (i.e., 30 and 90 °C). This outcome could be attributed to an increase in the NP clusters, higher heat absorption by the multiple NPs, and increased mixing capacity found in the high-concentration NFs. Moreover, at 90 °C, no substantial difference in the dynamic viscosity measurements was observed between the low- and high-concentration NF samples. Lastly, the tripartite hybrid based NF from sample 25, which was composed of 50% ZnO, 40% Al_2O_3, and 10% GO at 0.5 wt.% NF concentration, had an unusually high magnitude of dynamic viscosity at 75 °C.

4.1.4 Contact angle, ψ

The contact angle measurement of a lubrication fluid is necessary to determine the effect of the surface tension and wetness ability of the fluid for usage as a lubricant. The performance of the NF in an MQL system depends majorly on these properties for effective lubrication activity. In this work, the contact angle was measured using the edge inclination created by a droplet of each lubricant on a mirror-finished surface of the TC4 alloy.

Figure 14 shows the values of contact angles obtained in each NF sample based on the concentration of NPs in the fluid. The 1 wt.% concentration tripartite hybrid based NF sample exhibited the highest values of contact angle. The contact angle of the pure palm oil (α = 23.5°) increased by adding NPs into the oil. Furthermore, the results indicated that the tripartite hybrid Al_2O_3-based NF had the highest contact angle value compared with the other samples.

Considering the contact angle values in the monotype and tripartite hybrid NFs, the Al_2O_3-based NFs had the highest contact angles compared with the other NF compositions. As shown in Figs. 14(a)–14(c), the NF samples with compositions 50% Al_2O_3:40% ZnO:10% GO and 50% ZnO:40% Al_2O_3:10% GO produced similar results for the contact angle measurements at different NF concentrations. Palm oil with Al_2O_3 NF had better wettability than palm oil with GO and palm oil with ZnO NFs.

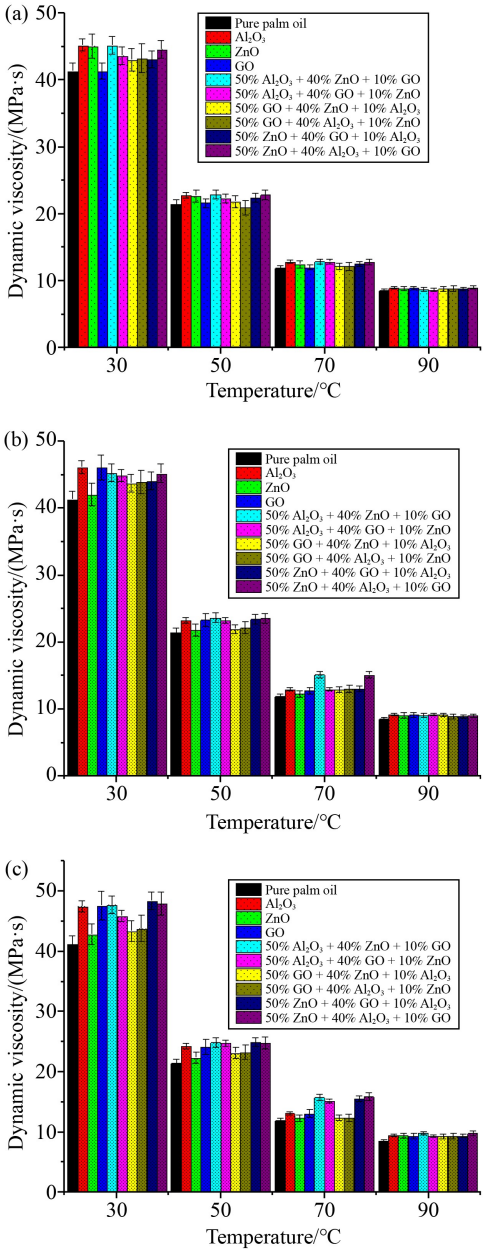

Fig. 13 Influence of NF concentration on dynamic viscosity: (a) 0.1%, (b) 0.5%, and (c) 1%.

Previous researchers have explained that the Al_2O_3-based NPs can create an unbalanced variation in the interacting forces between the NP and fluid, thereby increasing the wettability of the fluid [96,97]. This finding is evident from the results of the Al_2O_3-based NFs, where a positive effect on the contact angles was induced. Similarly, the 1% NF concentration of the tripartite hybrid NF had the highest magnitude of contact angles (Fig. 14(c)). The lowest contact angle was obtained in the pure oil and the GO NF samples. The effect of the NPs on the palm oil was not apparent in the low-concentration lubricants (0 to 0.5 wt.%). However, the measured contact angles drastically increased when

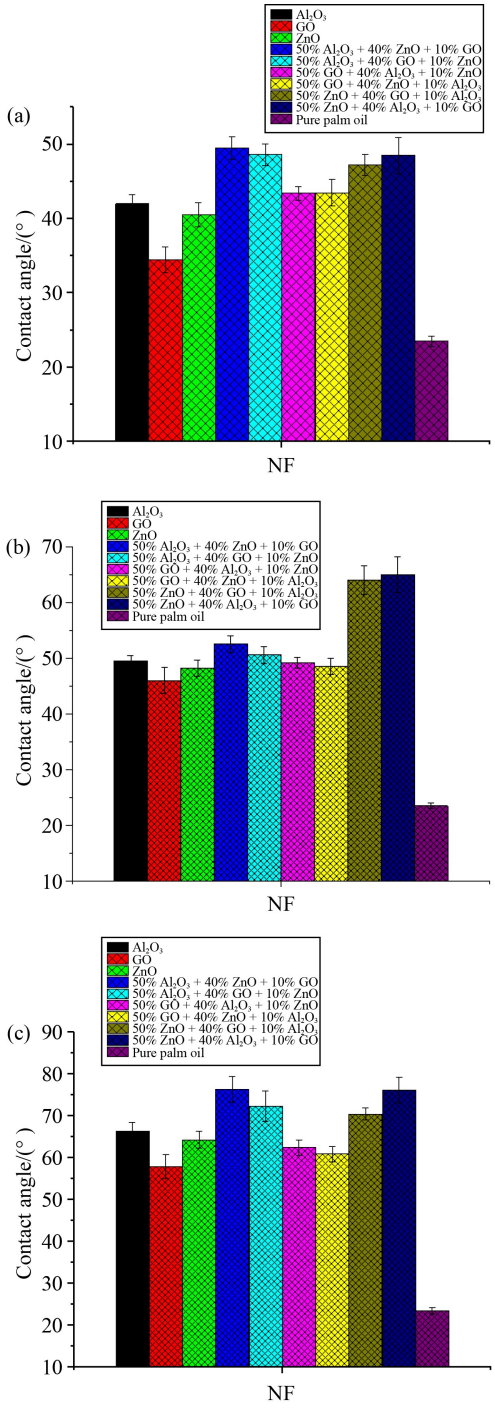

Fig. 14 Influence of NF concentration on contact angle: (a) 0.1%, (b) 0.5%, and (c) 1%.

the NF concentration was increased from 0.5% to 1%.

The 1% concentration tripartite hybrid NF had higher contact angles compared with the pure oil and monotype NFs. This enhancement can be explained by the higher surface tension caused by the interactions of the individual NPs with the mixed fluid. Moreover, the uneven rate of agglomeration of the individual NPs in the tripartite hybrid NF contributed to the improved spread/wetting capacity. Furthermore, explanations from previous works indicated that different types of NPs when mixed at higher NF concentrations led to an increase in the magnitude of the attractive Van der Waals forces within the fluid [49,98]. Equally, the increased inspissation realized in the tripartite hybrid NF sample No. 14 was due to the improved bonding rate of the individual NPs as a result of the suitable combination ratio.

Figure 15 compares the results for the measured contact angles in the pure palm oil and the NF. The result presentation was analyzed according to the dominant NPs present in the fluid. Finally, the best-performing NF samples in terms of contact angle measurements were the tripartite hybrid NF samples (14, 21, and 23).

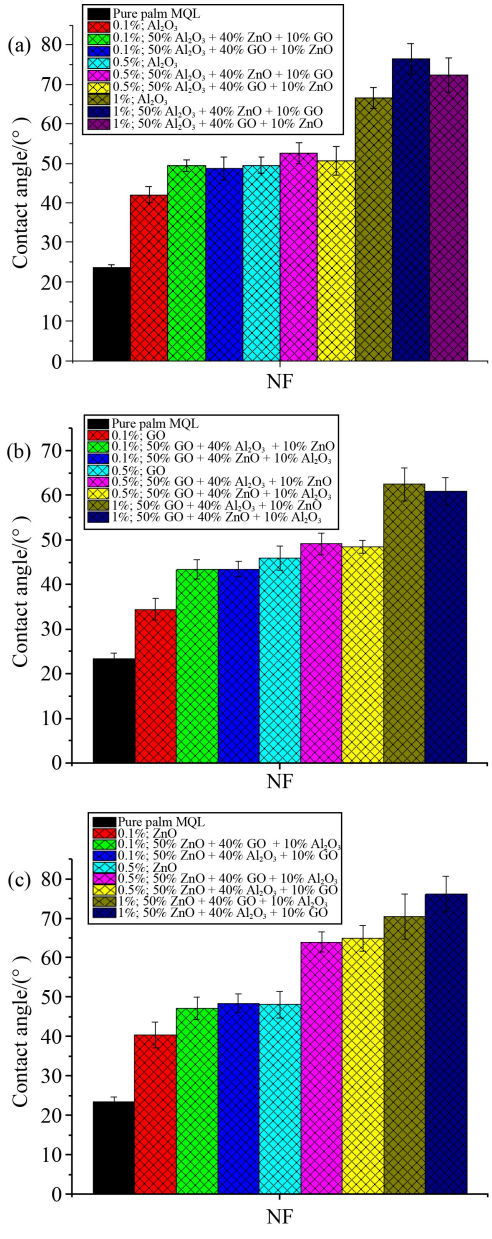

Fig. 15 Influence of different NF types on contact angle: (a) Al_2O_3 based, (b) GO based, and (c) ZnO based.

4.2 Grinding performance of the lubricants

The grinding operations were conducted on a TC4 alloy workpiece material using the same machine setting for each lubricant type to provide a basis for comparison in terms of performance between all the lubricant types. Because the 1 wt.% NF was the optimal NF concentration, the 1 wt.% concentration samples were used to conduct the experiments (sample types in Table 7). Likewise, the MQL variables and machine settings indicated in Table 6 were used to perform the grinding operations on the TC4 alloy workpiece material. The experimental results from the grinding experiments are explained in this section.

Table 7 Experimental settings for grinding tests

Experimental run	Parameter	
	NF concentration/wt.%	NF
1	0	Pure palm oil
2	1	Al_2O_3
3	1	GO
4	1	ZnO
5	1	50% Al_2O_3 + 40% ZnO + 10% GO
6	1	50% Al_2O_3 + 40% GO + 10% ZnO
7	1	50% GO + 40% Al_2O_3 + 10% ZnO
8	1	50% GO + 40% ZnO + 10% Al_2O_3
9	1	50% ZnO + 40% Al_2O_3 + 10% GO
10	1	50% ZnO + 40% GO + 10% Al_2O_3

4.2.1 Tangential and normal grinding forces and force ratio

Grinding forces are often used to demonstrate the performance of lubricants in grinding. A smaller magnitude of the grinding forces is more desirable because it indicates a lower amount of energy expended to remove a unit volume of the workpiece material. Hence, in MQL-based experiments, a lower grinding force indicates a better lubrication capacity of the lubricant [3,46,99–102]. The two types of forces predominant during grinding operations are the forces along the x and y axes, referred to as the tangential and normal grinding forces, respectively. The axial force, which is along the z-axis, is negligible.

An overview of the results obtained from the grinding experiments of this work indicated that the different MQL fluids expended different magnitudes of the tangential (f_t) and normal (f_n) grinding forces. The Al_2O_3-based tripartite hybrid NF sample from experimental run 5 in Table 7 exhibited the lowest amount of normal and tangential grinding forces. This result indicated a substantial decrease in the frictional forces and drag during the grinding operations. This result agreed with the results obtained in the preliminary tribological and thermophysical tests. Further, the tripartite hybrid based NFs generally had a lower grinding force compared with the pure palm oils in the MQL system. Additionally, the hierarchy of lubrication performance of the monotype NFs in descending order was Al_2O_3 > ZnO > GO.

Comparisons among the tripartite hybrid NFs indicated that the Al_2O_3-based lubricants produced lower values of grinding forces. The optimum NF sample, which was composed of 1 wt.% (50% Al_2O_3 + 40% ZnO + 10% GO), reduced the f_t and f_n by 41.5% and 30%, respectively, compared with the pure palm oil-based lubricant. The rates of reduction effected by each tripartite hybrid lubricant sample on f_t and f_n compared with the pure oil are illustrated in Figs. 16 and 17, respectively. The poor performance of the pure palm oil-based MQL system was due to the susceptibility of the molecules within the pure oil to be dislodged easily when under intense pressure. The tripartite hybrid based NFs can withstand the high pressure exerted by the grinding wheels. Moreover, the tripartite hybrid NFs that consisted of a higher amount of Al_2O_3 NPs exhibited lower grinding forces compared with the ZnO- and GO-based ones, which indicated a superior tribological performance of the Al_2O_3-based NF.

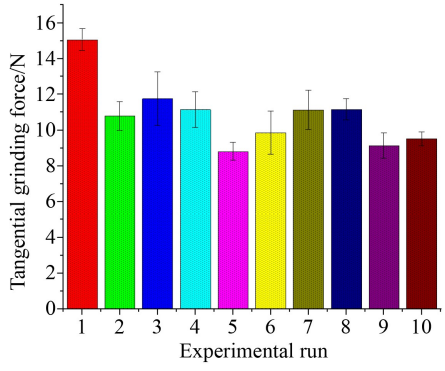

Fig. 16 Tangential grinding force f_t.

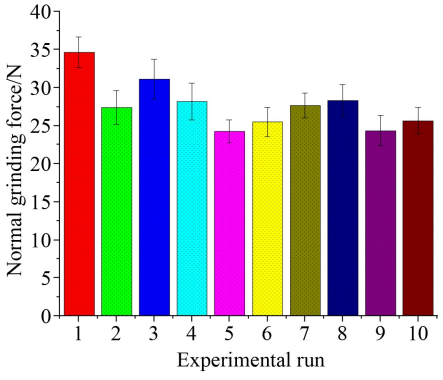

Fig. 17 Normal grinding force f_n.

Regarding the energy consumed during the grinding operations, a similar trend of the result obtained in the

tangential grinding forces was observed. The specific grinding energy is a function of the grinding power, meaning it is the amount of energy required to remove a unit material from the workpiece by a grinding wheel during the grinding operations. Most of the energy generated during the grinding operations is often lost in the form of heat, so achieving a sustainable machining involves reducing the specific grinding energy to the barest minimum. Hence, any lubricant that can obtain the lowest values of U exhibits the optimum lubrication capacity [12,103,104]. The NF samples from experimental runs 5 and 9 exhibited the lowest specific grinding energy. This result also indicates the superior lubricity of the tripartite hybrid NF produced using a higher amount of Al_2O_3 and ZnO NPs. Moreover, the monotype-based NF of these NPs presented a slightly higher amount of energy expended during the grinding operations. This result indicated the effectiveness of the hybrid NPs in improving the tribological and thermophysical performance of the lubricant.

Figure 18 shows the values of the specific grinding energy obtained from the grinding operations. The tripartite hybrid NFs generally decreased the magnitude of the specific grinding energy compared with pure palm oil. The hybrid NF, which consisted of 10% GO NP (experiment runs 5 and 9), expended the lowest amount of specific grinding energy. The results obtained showed that the tripartite hybrid NF if properly mixed can achieve about 40% reduction in the specific grinding energy compared with that when pure palm oil is used.

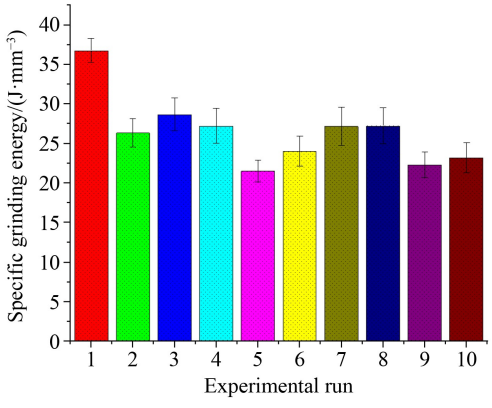

Fig. 18 Specific grinding energy U.

The grinding force ratio (frictional coefficient) is obtained by taking the ratio of f_t and f_n obtained from the grinding operation. It is one of the machining responses often used to quantify the lubricity of a lubricant in a material removal process [99,105,106]. The force ratio is also a measure of the frictional force between the wheel and the workpiece material. Any lubricant that exhibits a higher value of the force ratio is deemed to have poor lubricity. Therefore, a smaller value of the force ratio is more desired in any grinding operation. The results in Fig. 19 illustrate that the lowest grinding force ratio was achieved by sample 5, whereas the highest grinding force ratio was obtained by sample 1. Pure palm oil when used alone did not offer much reduction to the friction between the workpiece and the wheel. Moreover, the tripartite hybrid NF considerably reduced the grinding force ratio by 16.5%.

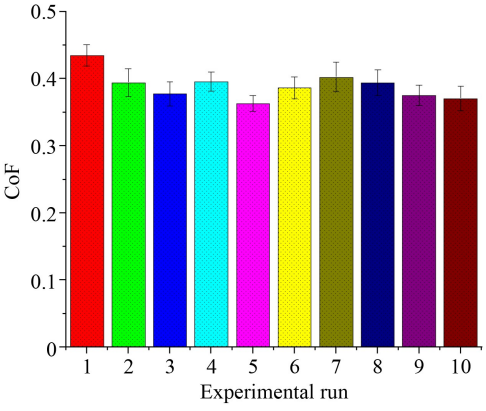

Fig. 19 Grinding force ratio μ.

4.2.2 Surface quality

The final surface quality of a machined component is a key component used to analyze the effectiveness of a machining system. The surface quality can be assessed qualitatively using SEM/visual analysis and quantitatively through surface roughness measurements.

To understand the source of the spikes on a workpiece material, during grinding operations, the grits on the grinding wheel were embedded into the workpiece material. Similarly, the grits on the grinding wheel were not uniformly distributed, and a larger part of the wheel was occupied by the softer bond material. In addition to factors such as chatter, friction, and excessive heat, this caused waviness and a nonuniform surface texture on the ground surface. The friction and continuous chopping of the work material by the grits encompassed the whole material removal and thereby created furrows and surface defects. Furthermore, grinding created a plastic deformation layer along the furrows of the grinding path and formed a rough top layer.

The performance of the grinding operation can then be evaluated quantitatively by measuring the surface roughness or qualitatively by visual microscopic analysis. Ra refers to the average magnitude of the miniature-sized ridges and spikes on the machined surface. Ra is measured by obtaining the arithmetic mean deviation of the surface of the ground component. Further, another roughness Rz can be obtained by comparing the average distance between the maximum peak and lowest valley point on the surface of the workpiece material. Hence, in

this section, the surface quality performance of lubricants using the Ra and Rz values of the machined sections is analyzed.

In this work, the average roughness (Ra and Rz) of the machined workpiece were obtained from roughness measurements taken along a defined plane in the grinding direction. The magnitude of the surface roughness was used to analyze roughness profiles of the ground TC4 material. The results of the surface roughness measurements for Ra and Rz in each experiment are given in Figs. 20(a) and 20(b), respectively. Furthermore, the surface morphology of the ground workpiece sections was analyzed qualitatively using the OLS-5000 laser microscope.

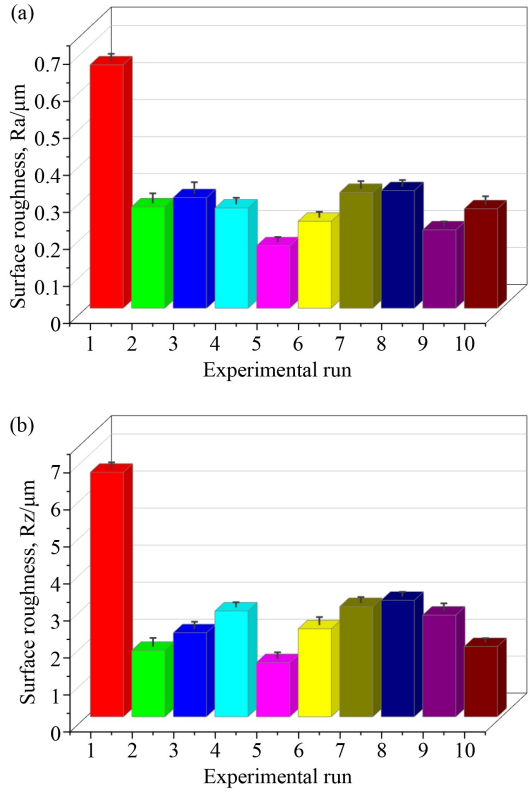

Fig. 20 Surface roughness measurements: (a) Ra and (b) Rz.

Figure 21 presents the microscopic results of the surface morphology in each of the ground samples. The tripartite hybrid NFs when used in MQL systems produced much superior surface quality compared with pure palm oil. The inferior lubrication capacity of the pure oil inflicted intense grinding damages such as grooves, wide ridges, pores, and burns on the workpiece material, as shown in the image of experimental run 1 (Fig. 21). Moreover, the different NF compositions exerted dissimilar capacities of lubrication on the grinding because the final texture of the ground components differed substantially from one another. In the monotype-based NFs, the Al_2O_3-based NFs presented a better surface finish with lower surface roughness values compared with the GO- and ZnO-based NFs. The hierarchy of surface quality performance in the monotype-based NFs in ascending order was GO < ZnO < Al_2O_3.

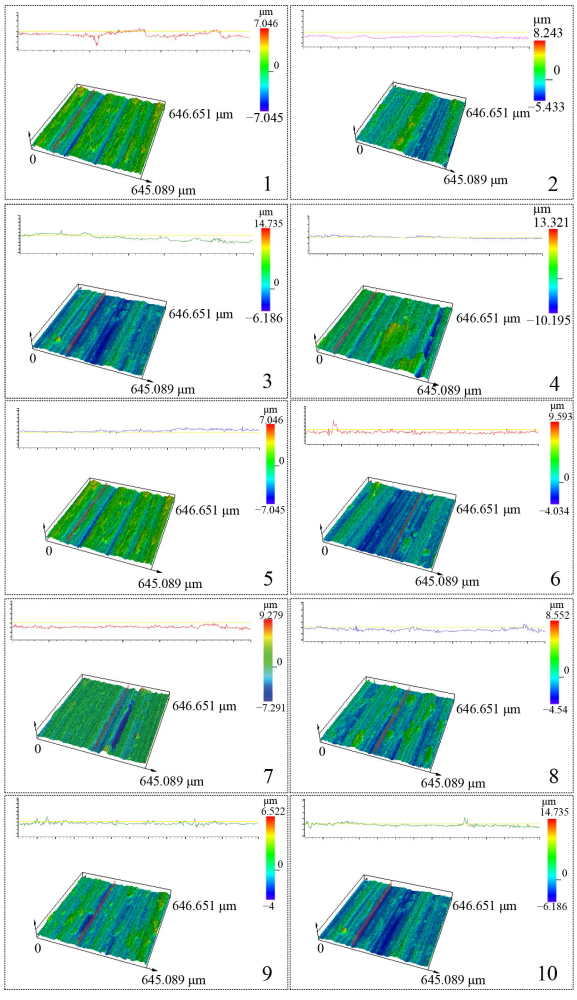

Fig. 21 Surface quality analysis with the 3D textural view of the ten machined parts. Bottom right number represents the experimental run number.

Additionally, a proper combination of the NF mixture in the tripartite hybrid NFs can substantially influence the surface quality of the machined parts. Likewise, an excess amount of the GO NPs in the NF caused lower lubrication performance of the MQL system. However, the surface quality of the samples machined using the Al_2O_3-based tripartite hybrid NF in MQL system had the least occurrence of surface deformations, and the lowest values of Ra and Rz.

The samples from experiments 5 and 9 produced the smoothest surfaces with the lowest surface roughness values of 0.169 and 0.212 μm, respectively. These results can be attributed to the layer of enhanced load-bearing capability of the tribofilm formed by these NFs. The formation of tribofilms by the vegetable-oil-based NFs has been explained by many researchers to be the reason

for excessive reduction of chatter, improved heat removal capacity, and low friction in MQL machining. Finally, the lubrication performance of the tripartite hybrid NFs in terms of surface quality responses in ascending order was GO-based NFs < ZnO-based NFs < Al_2O_3-based NFs. Hence, based on the findings, the composition of the tripartite hybrid NF should have the Al_2O_3 as the dominant NP.

Figure 22 presents the surface textures of the ground TC4-alloy workpiece material using different lubricants in the MQL system. The images were obtained using the SEM machine. As a result of the hardness of the CBN grits, many grinding-induced damages were noticeable on the machined surfaces. Surface damages such as wedges, micro/macro groves, fracturing/delamination, debris redeposition, and microwelds were apparent on the analyzed workpieces. For instance, the sample from experimental run 1, which was ground using pure palm oil in the MQL system, suffered severe delamination due to discontinuous motion existing in the grinding region. This result confirms the improper, ineffective lubrication and intense thermally-induced damage by the lubrication system.

Likewise, macrowelds were observed on the samples ground with pure palm oil. Additionally, the use of tripartite hybrid NF as the MQL lubricant considerably improved the surface quality of the ground workpiece. Due to their different compositions, each lubricant sample offered a distinctive surface outcome on the ground workpiece material. The tripartite hybrid NF remarkably improved the surface quality of the ground compared with those machined with monotype NF and pure palm oils. The samples ground with monotype-based NFs exhibited microplow marks, intense delamination, and exfoliations. However, a smoother surface was obtained in the workpieces ground with the ZnO- and Al_2O_3-based tripartite hybrid NFs. The superior surface quality of the components can be attributed to the tribological enhancement presented by the individual NPs in the tripartite hybrid NF. Equally, the GO-based tripartite hybrid NF produced the worst surface quality among all the developed tripartite hybrid NFs. The sample from experiment number 5 produced a smoother surface with minimum surface impairments compared with the remaining ground surfaces.

Figure 22 reveals the poor surface quality found in the

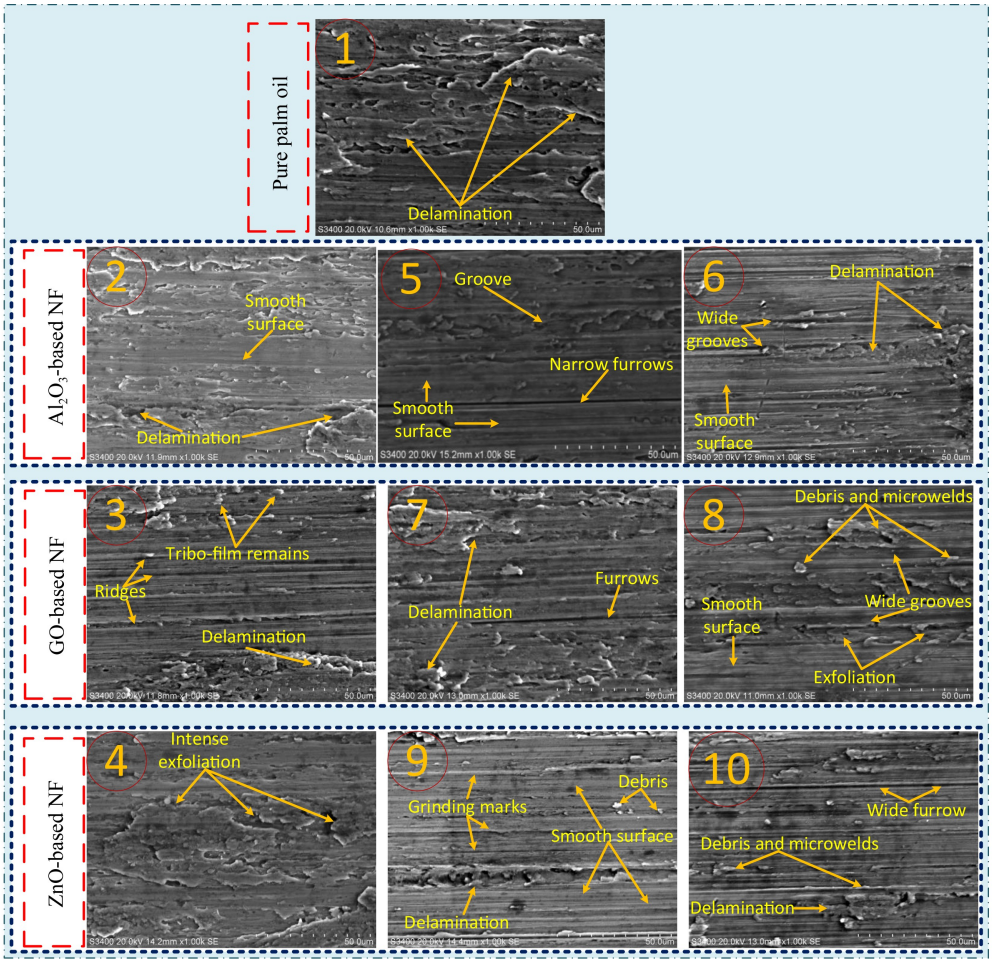

Fig. 22 SEM analysis of ground TC4-alloy workpiece using different lubricants in the MQL system.

samples from experiments 1, 3, 4, 7, 8, and 10 caused the high surface roughness in these experiments. This figure also indicates poor lubricity in the grinding operations. The Al_2O_3- and ZnO-based hybrid NFs produced a better surface finish. The improvement in the surface quality can be attributed to the higher wettability and lubricity of the tripartite hybrid NFs.

5 Conclusions

Recently, the utilization of infinitesimal amounts of lubricant through the MQL systems in the machining of advanced engineering materials has gained popularity due to the effectiveness and low cost offered by the MQL process. The system has been proven to be eco-friendly and efficient in grinding superhard engineering materials. Recent studies have shown that the use of NFs as the lubricant of the MQL system can further improve the overall machining performance of the lubrication system. The NF plays an important role in reducing friction and thermal loads around the machining/contact zone, and thereby improves machining efficiency and surface quality.

In this work, the novel uses of a tripartite hybrid NF manufactured using Al_2O_3, ZnO, and GO NPs are introduced. The hybrid NF was mixed in pure palm oil using a 5:4:1 mix ratio for the three NPs at different weight-percent concentrations of 0.1%, 0.5%, and 1%. Tribological and physical tests were conducted on each of the manufactured NF, and the results were compared with those of pure palm oil. The pure, monotype, and tripartite hybrid NFs were compared based on their dynamic viscosity at different temperatures, CoF, and wettability. Further, the optimum NF combination with superior tribological features was ascertained. Grinding tests were performed on a TC4 alloy using the lubricants with an MQL system. According to the results obtained, the following conclusions can be made:

1) Tripartite hybrid NF exhibited superior lubrication behavior compared with pure palm oil and monotype NFs.

2) Increasing the NP concentration from 0% to 1% caused a steady reduction in the friction between the ZrO_2 ball and TC4 alloy. Likewise, in the frictional tests, the wear on the ZrO_2 balls was much lower when the tripartite hybrid NFs were utilized. In the tribological test, the 1% NF concentration of the hybrid sample with a mix ratio of 50% Al_2O_3:40% ZnO:10% GO was the optimum composition because it exhibited the lowest frictional coefficient of 0.224.

3) The stability analysis showed that the Al_2O_3-based tripartite hybrid NF had the longest settling times among all the studied NFs.

4) In addition, the contact angles made by a droplet of each lubricant on the TC4 surface were used to investigate the wettability of the lubricants. The tripartite hybrid Al_2O_3 NF exhibited the highest contact angle compared with the pure oil, monotype NF, and the other tripartite NFs. The smallest and highest contact angles were measured in the pure oil sample and the hybrid sample with a mix ratio of 50% Al_2O_3:40% ZnO:10% GO. Similarly, the results obtained indicated that all the NFs had a higher contact angle than the pure oil. Hence, the hybrid NFs remarkably enhanced the wettability of palm.

5) In the Al_2O_3-based NFs, the 1% concentration tripartite hybrid NF produced using the NF composition of 50% Al_2O_3:40% ZnO:10% GO had the highest dynamic viscosity at different temperatures. Moreover, among the GO-based tripartite hybrid NF, the 1% concentration sample with a mix ratio of 50% GO:40% Al_2O_3:10% ZnO achieved the best results of dynamic viscosity. Similarly, regarding the ZnO-based NFs, the 1% concentration tripartite hybrid sample with NF mixture of 50% ZnO:40% Al_2O_3:10% GO obtained the highest results of dynamic viscosity. The Al_2O_3 NPs played an important role in improving the dynamic viscosity of the NFs because all the samples where it was dominant exhibited superior tribological behaviors. Finally, the dynamic viscosity of the tripartite-hybrid-based NFs increased by 12%, 5%, and 11.5% for the Al_2O_3-, GO-, and ZnO-based hybrid NFs compared with the pure oil samples, respectively.

6) The use of tripartite hybrid NF in the MQL system during grinding operations reduced the tangential and normal grinding forces by 41.5% and 30%, respectively, compared with the use of pure palm oil. This outcome indicated the enhanced lubrication capacity of the tripartite hybrid NFs. Similarly, compared with the pure palm oils, the tripartite hybrid based NF decreased the grinding force ratio and specific grinding energy by 16.5% and 40%, respectively.

7) In terms of surface quality, the Al_2O_3 monotype-based NFs produced a superior surface quality compared with the other monotype NFs and pure palm oil. The TC4 alloy workpiece machined using the tripartite hybrid based samples with mix ratios of 50% Al_2O_3:40% ZnO:10% GO and 50% ZnO:40% Al_2O_3:10% GO were the smoothest and exhibited the lowest surface roughness of 0.169 and 0.212 μm, respectively. The surface quality of the ground TC4 workpiece using the MQL system improved by 42%–71% compared with the samples machined with pure palm oil as the lubricant.

Researchers have mostly focused on the monotype and dual-based hybrid NFs as lubricants for MQL systems. However, in this work, a novel tripartite-based hybrid NF manufactured using Al_2O_3, GO, and ZnO NPs in a 50%:40%:10% mix-ratio is presented. Increasing the NF concentration enhanced the tribological behaviors of the NFs. An optimum NF combination was obtained, and grinding experiments were conducted on the TC4 alloy

with the MQL system. Our work extends from preparation, tribo-physical investigations, and novel application of the NFs in the grinding of TC4 alloys. The findings from our work can be useful for developing eco-friendly NFs with enhanced tribological performances, which are useful for machining advanced engineering materials with MQL systems. Lastly, further investigating the performance of the tripartite-based NFs in different compositions such as 70%:20%:10%, 60%:30%:10%, and 40%:30%:30% is recommended.

Nomenclature

Abbreviations

ASTM	American society for testing and materials
CA	Cooled air
CBN	Cubic boron nitride
CeO_2	Cerium oxide
CG	Conventional grinding
CNC	Computer numerical control
CoF	Coefficient of friction
CPG	Cylindrical plunge grinding
GO	Graphene oxide
MQL	Minimum quantity lubrication
MWCNT	Multi-walled carbon nanotube
NMQL	Nanofluid minimum quantity lubrication
NP	Nanoparticle
NF	Nanofluid
SEM	Scanning electron microscope
SiO_2	Silicon dioxide
SWCNT	Single-walled carbon nanotube
TC4	Titanium alloy (Ti-6Al-4V)
TiO_2	Titanium oxide
UL	Ultra low
UMT	Universal mechanical tester
UAG	Ultrasonic assisted grinding
ZnO	Zinc oxide
ZrO_2	Zirconia

Variables

a_e	Grinding depth
b	Wheel width
C_f	Correlation factor
d	MQL ejection distance
d_p	Diameter of NPs
f_n	Normal grinding force
f_t	Tangential grinding force
n	Predetermined variable
n_{NPs}	Number of NPs
N_A	Avogadro's number
P	Ejection pressure
Q_m	Droplet flow rate
R	Gas constant
Ra	Surface roughness parameter
Rz	Surface roughness parameter
T	Temperature
U	Specific grinding energy
v_s	Wheel speed
v_w	Feed rate
V_b	Wheel wear
V_B	Brownian velocity of particles
w_{nf}	Total weight percent of NF
w_{np}	Total weight percent of individual NP
w_{NPs}	Total weight percent of NPs
w_{oil}	Total weight percent of base oil (i.e., palm oil)
w_{surf}	Total weight percent of surfactant and anti-oxidant
α	Transpose of the coefficient of solid phase
μ_{bf}	Viscosity of base fluid
μ_{nf}	Viscosity of NF
δ	Average distance between the NPs
ψ	Contact angle
Ψ	Volume concentration of NPs
ρ_{NPs}	Density of NPs
ρ_{oil}	Density of oil/fluid
ρ_p	Density of NP
ρ_{surf}	Density of surfactant
Σ	Residual stress

Acknowledgements This study was financially supported by the National Natural Science Foundation of China (Grant Nos. 52305477, 52375447, 52305474, and 52205481), the Major Special Projects of Aero-engine and Gas Turbine, China (Grant No. 2017-VII-0002-0095), the Natural Science Foundation of Jiangsu Province, China (Grant No. BK20210407), the Special Fund of Taishan Scholars Project, China (Grant No. tsqn202211179), the Youth Talent Promotion Project in Shandong, China (Grant No. SDAST2021qt12), Qingdao Postdoctoral Researchers Applied Research Project, China (Grant No. QDBSH20230102050), the Support plan for Outstanding Youth Innovation Team in Universities of Shandong Province, China (Grant No. 2023KJ114), and Qingdao Science and Technology Planning Park Cultivation Plan (Grant No. 23-1-5-yqpy-17-qy).

Conflict of Interest Changhe LI is a member of the Editorial Board of *Frontiers of Mechanical Engineering*, who was excluded from the peer review and all editorial decisions related to the acceptance and publication of this article. Peer review was handled independently by the other editors to minimize bias.

References

1. Lv T, Xu X F, Weng H Z, Yu A B, Niu C C, Hu X D. A study on lubrication and cooling performance and machining characteristics of magnetic field–assisted minimum quantity lubrication using Fe_3O_4 nanofluid as cutting fluid. The International Journal of Advanced Manufacturing Technology, 2022, 123(11–12): 3857–3869
2. Lv T, Xu X F, Yu A B, Niu C C, Hu X D. Ambient air quantity and cutting performances of water-based Fe_3O_4 nanofluid in magnetic minimum quantity lubrication. The International Journal of Advanced Manufacturing Technology, 2021, 115(5–6): 1711–1722
3. Dambatta Y S, Li C H, Yang M, Beikai L I, Gao T, Liu M Z, Cui X, Wang X M, Zhang Y B, Said Z, Sharma S, Zhou Z M. Grinding with minimum quantity lubrication: a comparative assessment. The International Journal of Advanced Manufacturing Technology, 2023, 128(3–4): 955–1014
4. Sartori S, Ghiotti A, Bruschi S. Solid lubricant-assisted minimum quantity lubrication and cooling strategies to improve Ti-6Al-4V machinability in finishing turning. Tribology International, 2018, 118: 287–294
5. Yıldırım Ç V. Experimental comparison of the performance of nanofluids, cryogenic and hybrid cooling in turning of Inconel 625. Tribology International, 2019, 137: 366–378
6. Singh H, Sharma V S, Dogra M. Exploration of graphene assisted vegetables oil based minimum quantity lubrication for surface grinding of Ti-6Al-4V-ELI. Tribology International, 2020, 144: 106113
7. Lv T, Xu X F, Yu A B, Hu X D. Oil mist concentration and machining characteristics of SiO_2 water-based nano-lubricants in electrostatic minimum quantity lubrication-EMQL milling. Journal of Materials Processing Technology, 2021, 290: 116964
8. Cui X, Li C H, Zhang Y B, Said Z, Debnath S, Sharma S, Ali H M, Yang M, Gao T, Li R Z. Grindability of titanium alloy using cryogenic nanolubricant minimum quantity lubrication. Journal of Manufacturing Processes, 2022, 80: 273–286
9. Jamil M, Khan A M, Hegab H, Gong L, Mia M, Gupta M K, He N. Effects of hybrid Al_2O_3-CNT nanofluids and cryogenic cooling on machining of Ti-6Al-4V. The International Journal of Advanced Manufacturing Technology, 2019, 102(9–12): 3895–3909
10. Zaman P B, Tusar M I H, Dhar N R. Selection of appropriate process inputs for turning Ti-6Al-4V alloy under hybrid Al_2O_3-MWCNT nano-fluid based MQL. Advances in Materials and Processing Technologies, 2022, 8(1): 380–400
11. Zhang G F, Luo D J, Wu G C, Liu D, Wang J K, Deng X, Cai J B. Effect of carbon nanotubes intensified coolant on the grinding performance of carburizing and quenching 12Cr2Ni4A steel. The International Journal of Advanced Manufacturing Technology, 2023, 124(11–12): 3935–3946
12. Zhang D K, Li C H, Jia D Z, Zhang Y B, Zhang X W. Specific grinding energy and surface roughness of nanoparticle jet minimum quantity lubrication in grinding. Chinese Journal of Aeronautics, 2015, 28(2): 570–581
13. Zhang X P, Li C H, Jia D Z, Gao T, Zhang Y B, Yang M, Li R Z, Han Z G, Ji H J. Spraying parameter optimization and microtopography evaluation in nanofluid minimum quantity lubrication grinding. The International Journal of Advanced Manufacturing Technology, 2019, 103(5–8): 2523–2539
14. Peng R T, He X B, Tong J W, Tang X Z, Wu Y P. Investigation on suspension stability and anti-wear and anti-friction properties of soybean oil based Al_2O_3 nanofluid. Journal of Functional Materials, 2020, 51(8): 194–199
15. Alshehhi A A, Said Z, Sohail M A. Rheological behavior of hybrid nanofluids. In: Said Z ed. Hybrid Nanofluids: Preparation, Characterization and Applications, 2022: 111–129
16. Ranga Babu J A, Kumar K K, Rao S S. State-of-art review on hybrid nanofluids. Renewable & Sustainable Energy Reviews, 2017, 77: 551–565
17. Barewar S D, Kotwani A, Chougule S S, Unune D R. Investigating a novel Ag/ZnO based hybrid nanofluid for sustainable machining of inconel 718 under nanofluid based minimum quantity lubrication. Journal of Manufacturing Processes, 2021, 66: 313–324
18. Cakmak N K, Said Z, Sundar L S, Ali Z M, Tiwari A K. Preparation, characterization, stability, and thermal conductivity of rGO-Fe_3O_4-TiO_2 hybrid nanofluid: an experimental study. Powder Technology, 2020, 372: 235–245
19. Junankar A A, Parate S R, Dethe P K, Dhote N R, Gadkar D G, Gadkar D D, Gajbhiye S A. A review: enhancement of turning process performance by effective utilization of hybrid nanofluid and MQL. Materials Today, 2021, 38: 44–47
20. Lv T, Yu A B, Jin G Y, Xu X F. Aerosol characteristics and turning performance of magnetic minimum quantity lubrication. Multiphase Science and Technology, 2022, 34(4): 57–73
21. Kumar A, Ghosh S, Aravindan S. Experimental investigations on surface grinding of silicon nitride subjected to mono and hybrid nanofluids. Ceramics International, 2019, 45(14): 17447–17466
22. Sharma A K, Tiwari A K, Dixit A R, Singh R K. Hybrid Nanoparticles Enriched Cutting Fluids in Machining Processes. Nanofluids and their Engineering Applications. Boca Raton: CRC Press, 2019
23. Zhang X P, Li C H, Zhang Y B, Jia D Z, Li B K, Wang Y G, Yang M, Hou Y L, Zhang X W. Performances of Al_2O_3/SiC hybrid nanofluids in minimum-quantity lubrication grinding. The International Journal of Advanced Manufacturing Technology, 2016, 86(9–12): 3427–3441
24. Zhang X P, Li C H, Zhang Y B, Wang Y G, Li B K, Yang M, Guo S M, Liu G T, Zhang N Q. Lubricating property of MQL

grinding of Al_2O_3/SiC mixed nanofluid with different particle sizes and microtopography analysis by cross-correlation. Precision Engineering, 2017, 47: 532–545

25. Duc T M, Long T T, Tuan N M. Novel uses of Al_2O_3/MoS_2 hybrid nanofluid in MQCL hard milling of hardox 500 steel. Lubricants, 2021, 9(4): 45
26. Jamil M, He N, Zhao W, Khan A M, Laghari R A. Tribology and machinability performance of hybrid Al_2O_3-MWCNTs nanofluids-assisted MQL for milling Ti-6Al-4V. The International Journal of Advanced Manufacturing Technology, 2022, 119(3–4): 2127–2144
27. Kashyap D P, Vardhan S, Dogra M, Singh R. Exploration of Ti6Al4V surface grinding under dry and MQL environments. International Journal of Applied Science and Engineering, 2022, 19(2): 1–5
28. Kalita P, Malshe A, Jiang W P, Shih A. Tribological study of nano lubricant integrated soybean oil for minimum quantity lubrication (MQL) grinding. Transactions of NAMRI/SME, 2010, 38(313): 137–144
29. Hemmat Esfe M, Esfandeh S, Saedodin S, Rostamian H. Experimental evaluation, sensitivity analyzation and ANN modeling of thermal conductivity of ZnO-MWCNT/EG-water hybrid nanofluid for engineering applications. Applied Thermal Engineering, 2017, 125: 673–685
30. Wole-Osho I, Okonkwo E C, Kavaz D, Abbasoglu S. An experimental investigation into the effect of particle mixture ratio on specific heat capacity and dynamic viscosity of Al_2O_3-ZnO hybrid nanofluids. Powder Technology, 2020, 363: 699–716
31. Hemmat Esfe M, Behbahani P M, Arani A A A, Sarlak M R. Thermal conductivity enhancement of SiO_2–MWCNT (85: 15%)–EG hybrid nanofluids: ANN designing, experimental investigation, cost performance and sensitivity analysis. Journal of Thermal Analysis and Calorimetry, 2017, 128(1): 249–258
32. Bahari N M, Che Mohamed Hussein S N, Othman N H. Synthesis of Al_2O_3–SiO_2/water hybrid nanofluids and effects of surfactant toward dispersion and stability. Particulate Science and Technology, 2021, 39(7): 844–858
33. Aravind S S J, Ramaprabhu S. Graphene–multiwalled carbon nanotube-based nanofluids for improved heat dissipation. RSC Advances, 2013, 3(13): 4199–4206
34. Singh R K, Sharma A K, Dixit A R, Tiwari A K, Pramanik A, Mandal A. Performance evaluation of alumina-graphene hybrid nano-cutting fluid in hard turning. Journal of Cleaner Production, 2017, 162: 830–845
35. Amirthalingam S, Thangavel B. On the thermal conductivity and viscosity of bionanofluid with neem (Azadirachta indica) assisted zinc oxide nanoparticles. Journal of Thermal Science and Technology, 2020, 15(3): JTST0023
36. Lee P H, Nam J S, Li C J, Lee S W. An experimental study on micro-grinding process with nanofluid minimum quantity lubrication (MQL). International Journal of Precision Engineering and Manufacturing, 2012, 13(3): 331–338
37. Mao C, Tang X J, Zou H F, Huang X M, Zhou Z X. Investigation of grinding characteristic using nanofluid minimum quantity lubrication. International Journal of Precision Engineering and Manufacturing, 2012, 13(10): 1745–1752
38. Thakur A, Manna A, Samir S. Experimental investigation of nanofluids in minimum quantity lubrication during turning of EN-24 steel. Proceedings of the Institution of Mechanical Engineers, Part J: Journal of Engineering Tribology, 2020, 234(5): 712–729
39. Jyothirmayee Aravind S S, Ramaprabhu S. Graphene wrapped multiwalled carbon nanotubes dispersed nanofluids for heat transfer applications. Journal of Applied Physics, 2012, 112(12): 124304
40. Al-Rashed A A A A, Ranjbarzadeh R, Aghakhani S, Soltanimehr M, Afrand M, Nguyen T K. Entropy generation of boehmite alumina nanofluid flow through a minichannel heat exchanger considering nanoparticle shape effect. Physica A: Statistical Mechanics and its Applications, 2019, 521: 724–736
41. Esfahani M R, Languri E M, Nunna M R. Effect of particle size and viscosity on thermal conductivity enhancement of graphene oxide nanofluid. International Communications in Heat and Mass Transfer, 2016, 76: 308–315
42. Zhang Y B, Li C H, Jia D Z, Zhang D K, Zhang X W. Experimental evaluation of the lubrication performance of MoS_2/CNT nanofluid for minimal quantity lubrication in Ni-based alloy grinding. International Journal of Machine Tools & Manufacture, 2015, 99: 19–33
43. Shen B, Shih A J, Tung S C. Application of nanofluids in minimum quantity lubrication grinding. Tribology Transactions, 2008, 51(6): 730–737
44. Hernández Battez A, González R, Viesca J L, Fernández J E, Díaz Fernández J M, Machado A, Chou R, Riba J. CuO, ZrO_2 and ZnO nanoparticles as antiwear additive in oil lubricants. Wear, 2008, 265(3–4): 422–428
45. Li L. Research on the tribological properties of mixtures of nano-particles of CeO_2 and TiO_2 as lubricating oil additives. Marine Technology, 2007, 5: 41–43
46. Chu A X, Li C H, Zhou Z M, Liu B, Zhang Y B, Yang M, Gao T, Liu M Z, Zhang N Q, Dambatta Y S, Sharma S. Nanofluids minimal quantity lubrication machining: from mechanisms to application. Lubricants, 2023, 11(10): 422
47. Li C H. Effects of Nanofluid Concentration on Heat Transfer Performances in Cryogenic Nanofluid Minimum Quantity Lubrication Grinding. Thermodynamic Mechanism of MQL Grinding with Nano Bio-lubricant. Singapore: Springer, 2024, 299–309
48. Afshari F, Tuncer A D, Sözen A, Variyenli H I, Khanlari A, Gürbüz E Y. A comprehensive survey on utilization of hybrid nanofluid in plate heat exchanger with various number of plates. International Journal of Numerical Methods for Heat & Fluid Flow, 2022, 32(1): 241–264
49. Babar H, Ali H M. Towards hybrid nanofluids: preparation, thermophysical properties, applications, and challenges. Journal of Molecular Liquids, 2019, 281: 598–633
50. Hemmat Esfe M, Wongwises S, Naderi A, Asadi A, Safaei M R, Rostamian H, Dahari M, Karimipour A. Thermal conductivity of Cu/TiO_2–water/EG hybrid nanofluid: experimental data and modeling using artificial neural network and correlation. International Communications in Heat and Mass Transfer, 2015, 66: 100–104
51. Wu P, Chen X C, Zhang C H, Luo J B. Synergistic tribological

behaviors of graphene oxide and nanodiamond as lubricating additives in water. Tribology International, 2019, 132: 177–184
52. Gara L, Zou Q. Friction and wear characteristics of water-based ZnO and Al_2O_3 nanofluids. Tribology Transactions, 2012, 55(3): 345–350
53. Singh H, Sharma V S, Singh S, Dogra M. Nanofluids assisted environmental friendly lubricating strategies for the surface grinding of titanium alloy: Ti6Al4V-ELI. Journal of Manufacturing Processes, 2019, 39: 241–249
54. Mukhopadhyay M, Kundu P K. Ecological and economical processing of Ti-6Al-4V with an augmentation in grindability. Sādhanā, 2021, 46(4): 196
55. Guo Y B, Yen D W. Hard turning versus grinding—the effect of process-induced residual stress on rolling contact. Wear, 2004, 256(3–4): 393–399
56. Madarkar R, Agarwal S, Attar P, Ghosh S, Rao P V. Application of ultrasonic vibration assisted MQL in grinding of Ti-6Al-4V. Materials and Manufacturing Processes, 2018, 33(13): 1445–1452
57. Sadeghi M H, Haddad M J, Tawakoli T, Emami M. Minimal quantity lubrication-MQL in grinding of Ti-6Al-4V titanium alloy. The International Journal of Advanced Manufacturing Technology, 2009, 44(5–6): 487–500
58. Kacalak W, Lipiński D, Bałasz B, Rypina Ł, Tandecka K, Szafraniec F. Performance evaluation of the grinding wheel with aggregates of grains in grinding of Ti-6Al-4V titanium alloy. The International Journal of Advanced Manufacturing Technology, 2018, 94(1–4): 301–314
59. Abbas A T, Gupta M K, Soliman M S, Mia M, Hegab H, Luqman M, Pimenov D Y. Sustainability assessment associated with surface roughness and power consumption characteristics in nanofluid MQL-assisted turning of AISI 1045 steel. The International Journal of Advanced Manufacturing Technology, 2019, 105(1–4): 1311–1327
60. Zhang J C, Li C H, Zhang Y B, Yang M, Jia D Z, Liu G T, Hou Y L, Li R Z, Zhang N Q, Wu Q D, Cao H J. Experimental assessment of an environmentally friendly grinding process using nanofluid minimum quantity lubrication with cryogenic air. Journal of Cleaner Production, 2018, 193: 236–248
61. Ibrahim A M M, Li W, Xiao H, Zeng Z X, Ren Y H, Alsoufi M S. Energy conservation and environmental sustainability during grinding operation of Ti-6Al-4V alloys via eco-friendly oil/graphene nano additive and Minimum quantity lubrication. Tribology International, 2020, 150: 106387
62. Wang Y G, Li C H, Zhang Y B, Yang M, Li B K, Dong L, Wang J. Processing characteristics of vegetable oil-based nanofluid MQL for grinding different workpiece materials. International Journal of Precision Engineering and Manufacturing-Green Technology, 2018, 5(2): 327–339
63. Dambatta Y S, Sayuti M, Sarhan A A D, Hamdi M, Manladan S M, Reddy M. Tribological performance of SiO_2-based nanofluids in minimum quantity lubrication grinding of Si3N4 ceramic. Journal of Manufacturing Processes, 2019, 41: 135–147
64. Seid Ahmed Y, González L W H. Ti6Al4V grinding using different lubrication modes for minimizing energy consumption. The International Journal of Advanced Manufacturing Technology, 2023, 126(5–6): 2387–2405
65. Zhang J C, Wu W T, Li C H, Yang M, Zhang Y B, Jia D Z, Hou Y L, Li R Z, Cao H J, Ali H M. Convective heat transfer coefficient model under nanofluid minimum quantity lubrication coupled with cryogenic air grinding Ti-6Al-4V. International Journal of Precision Engineering and Manufacturing-Green Technology, 2021, 8(4): 1113–1135
66. Lopes J C, Garcia M V, Valentim M, Javaroni R L, Ribeiro F S F, de Angelo Sanchez L E, de Mello H J, Aguiar P R, Bianchi E C. Grinding performance using variants of the MQL technique: MQL with cooled air and MQL simultaneous to the wheel cleaning jet. The International Journal of Advanced Manufacturing Technology, 2019, 105(10): 4429–4442
67. de Moraes D L, Lopes J C, Andrioli B V, Moretti G B, da Silva A E, da Silva J M M, Ribeiro F S F, de Aguiar P R, Bianchi E C. Advances in precision manufacturing towards eco-friendly grinding process by applying MQL with cold air compared with cooled wheel cleaning jet. The International Journal of Advanced Manufacturing Technology, 2021, 113(11–12): 3329–3342
68. Liu M Z, Li C H, An Q L, Zhang Y B, Yang M, Cui X, Gao T, Dambatta Y S, Li R Z. Atomized droplets liquid film thickness model and verification in sustainable hybrid lubrication (Cryo-MQL) grinding. Friction, 2024 (in press) doi: 10.2139/ssrn.4735225
69. Dambatta Y S, Li C H, Sayuti M, Sarhan A A D, Yang M, Li B K, Chu A X, Liu M Z, Zhang Y B, Said Z, Zhou Z M. Grindability evaluation of ultrasonic assisted grinding of silicon nitride ceramic using minimum quantity lubrication based SiO_2 nanofluid. Chinese Journal of Mechanical Engineering, 2024, 37(1): 25
70. Sharma A K, Tiwari A K, Dixit A R, Singh R K, Singh M. Novel uses of alumina/graphene hybrid nanoparticle additives for improved tribological properties of lubricant in turning operation. Tribology International, 2018, 119: 99–111
71. Liu L Z, Zhang J F, Zhao J J, Liu F. Mechanical properties of graphene oxides. Nanoscale, 2012, 4(19): 5910–5916
72. Druffel T, Buazza O, Lattis M, Farmer S, Spencer M, Mandzy N, Grulke E A. The role of nanoparticles in visible transparent nanocomposites. In: Gaburro Z, Cabrini S, Talapin D, eds. Nanophotonic Materials V. San Diego: SPIE, 2008, 70300F
73. Konkena B, Vasudevan S. Understanding aqueous dispersibility of graphene oxide and reduced graphene oxide through pK_a measurements. The Journal of Physical Chemistry Letters, 2012, 3(7): 867–872
74. Luo C X, Liu J K, Lu Y, Du C S. Controllable preparation and sterilization activity of zinc aluminium oxide nanoparticles. Materials Science and Engineering: C, 2012, 32(4): 680–684
75. Luo J, Liu J, Yao H Y, Li Z H, Wei J C. An efficient method to improve the dispersion and biocompatibility of ZnO nanoparticles. Journal of Dispersion Science and Technology, 2023 (in press)
76. Schoff C K. Wettability phenomena and coatings. In: Schrader M E, Loeb G I, eds. Modern Approaches to Wettability: Theory and Applications. Boston: Springer, 1992, 375–395
77. Einstein A. A new determination of molecular dimensions. Annals of Physics, 1906, 19: 289–306
78. Batchelor G K. The effect of brownian motion on the bulk stress

in a suspension of spherical particles. Journal of Fluid Mechanics, 1977, 83(1): 97–117

79. Masoumi N, Sohrabi N, Behzadmehr A. A new model for calculating the effective viscosity of nanofluids. Journal of Physics D: Applied Physics, 2009, 42(5): 055501
80. Udawattha D S, Narayana M, Wijayarathne U P L. Predicting the effective viscosity of nanofluids based on the rheology of suspensions of solid particles. Journal of King Saud University - Science, 2019, 31(3): 412–426
81. Gholizadeh M, Jamei M, Ahmadianfar I, Pourrajab R. Prediction of nanofluids viscosity using random forest (RF) approach. Chemometrics and Intelligent Laboratory Systems, 2020, 201: 104010
82. Wu L S, Ek M, Song M H, Du S C. The effect of solid particles on liquid viscosity. Steel Research International, 2011, 82(4): 388–397
83. Kondratiev A, Jak E. Modeling of viscosities of the partly crystallized slags in the Al_2O_3-CaO-"FeO"-SiO_2 system. Metallurgical and Materials Transactions B, 2001, 32(6): 1027–1032
84. Ślęzak M. Mathematical models for calculating the value of dynamic viscosity of a liquid. Archives of Metallurgy and Materials, 2015, 60(2): 581–589
85. Jia D Z, Zhang N Q, Liu B, Zhou Z M, Wang X P, Zhang Y B, Mao C, Li C H. Particle size distribution characteristics of electrostatic minimum quantity lubrication and grinding surface quality evaluation. Diamond & Abrasives Engineering, 2021, 41(3): 89–95
86. Li B K, Li C H, Zhang Y B, Wang Y G, Yang M, Jia D Z, Zhang N Q, Wu Q D. Effect of the physical properties of different vegetable oil-based nanofluids on MQLC grinding temperature of Ni-based alloy. The International Journal of Advanced Manufacturing Technology, 2017, 89(9–12): 3459–3474
87. Shavit U, Chigier N. The role of dynamic surface tension in air assist atomization. Physics of Fluids, 1995, 7(1): 24–33
88. Krainer S, Hirn U. Contact angle measurement on porous substrates: effect of liquid absorption and drop size. Colloids and Surfaces A: Physicochemical and Engineering Aspects, 2021, 619: 126503
89. Singh J, Singh Chatha S. Tribological behaviour of nanofluids under minimum quantity lubrication in turning of AISI 1055 steel. Materials Today: Proceedings, 2021, 41: 825–832
90. Urmi W, Rahman M M, Hamzah W A W. An experimental investigation on the thermophysical properties of 40% ethylene glycol based TiO_2-Al_2O_3 hybrid nanofluids. International Communications in Heat and Mass Transfer, 2020, 116: 104663
91. Nabil M F, Azmi W H, Hamid K A, Mamat R. Experimental investigation of heat transfer and friction factor of TiO_2-SiO_2 nanofluids in water: ethylene glycol mixture. International Journal of Heat and Mass Transfer, 2018, 124: 1361–1369
92. Sharma A K, Singh R K, Dixit A R, Tiwari A K. Novel uses of alumina-MoS_2 hybrid nanoparticle enriched cutting fluid in hard turning of AISI 304 steel. Journal of Manufacturing Processes, 2017, 30: 467–482
93. Nazari Moghaddam R, Bahramian A, Fakhroueian Z, Karimi A, Arya S. Comparative study of using nanoparticles for enhanced oil recovery: wettability alteration of carbonate rocks. Energy & Fuels, 2015, 29(4): 2111–2119
94. Dai W, Kheireddin B, Gao H, Liang H. Roles of nanoparticles in oil lubrication. Tribology International, 2016, 102: 88–98
95. Singh Y, Kumar Singh N, Sharma A, Singla A, Singh D, Abd Rahim E. Effect of ZnO nanoparticles concentration as additives to the epoxidized Euphorbia Lathyris oil and their tribological characterization. Fuel, 2021, 285: 119148
96. Cieśliński J T, Krygier K A. Sessile droplet contact angle of water–Al_2O_3, water–TiO_2 and water–Cu nanofluids. Experimental Thermal and Fluid Science, 2014, 59: 258–263
97. Vafaei S, Borca-Tasciuc T, Podowski M Z, Purkayastha A, Ramanath G, Ajayan P M. Effect of nanoparticles on sessile droplet contact angle. Nanotechnology, 2006, 17(10): 2523
98. Bhuiyan M H U, Saidur R, Mostafizur R M, Mahbubul I M, Amalina M A. Experimental investigation on surface tension of metal oxide–water nanofluids. International Communications in Heat and Mass Transfer, 2015, 65: 82–88
99. Dambatta Y S, Sayuti M, Sarhan A A D, Ab Shukor H B, Derahman N A, Manladan S M. Prediction of specific grinding forces and surface roughness in machining of AL6061–T6 alloy using ANFIS technique. Industrial Lubrication and Tribology, 2019, 71(2): 309–317
100. Liu M Z, Li C H, Zhang Y B, Yang M, Gao T, Cui X, Wang X M, Xu W H, Zhou Z M, Liu B, Said Z, Li R Z, Sharma S. Analysis of grinding mechanics and improved grinding force model based on randomized grain geometric characteristics. Chinese Journal of Aeronautics, 2023, 36(7): 160–193
101. Sui M H, Li C H, Wu W T, Yang M, Ali H M, Zhang Y B, Jia D Z, Hou Y L, Li R Z, Cao H J. Temperature of grinding carbide with castor oil-based MoS_2 nanofluid minimum quantity lubrication. Journal of Thermal Science and Engineering Applications, 2021, 13(5): 051001
102. Wang X M, Song Y X, Li C H, Zhang Y B, Ali H M, Sharma S, Li R Z, Yang M, Gao T, Liu M Z, Cui X, Said Z, Zhou Z M. Nanofluids application in machining: a comprehensive review. The International Journal of Advanced Manufacturing Technology, 2024, 131(5): 3113–3164
103. Jia D Z, Zhang Y B, Li C H, Yang M, Gao T, Said Z, Sharma S. Lubrication-enhanced mechanisms of titanium alloy grinding using lecithin biolubricant. Tribology International, 2022, 169: 107461
104. Xu W H, Li C H, Cui X, Zhang Y B, Yang M, Gao T, Liu M Z, Wang X M, Zhou Z M, Sharma S, Dambatta Y S. Atomization mechanism and machinability evaluation with electrically charged nanolubricant grinding of GH4169. Journal of Manufacturing Processes, 2023, 106: 480–493
105. K M K, Ghosh A. On grinding force ratio, specific energy, G-ratio and residual stress in SQCL assisted grinding using aerosol of MWCNT nanofluid. Machining Science and Technology, 2021, 25(4): 585–607
106. Dambatta Y S, Sarhan A A D, Sayuti M B A K, Shukor M H B A. Fuzzy logic method to investigate grinding of alumina ceramic using minimum quantity lubrication. International Journal of Applied Ceramic Technology, 2019, 16(4): 1668–1683